Study of Correlation Between EEG Electrodes for the Analysis of Cortical Responses Related to Binaural Hearing

EVA IGNATIOUS, **SAMI AZAM**, (Member, IEEE), **MIRJAM JONKMAN**, (Member, IEEE), **AND FRISO DE BOER**

College of Engineering, IT and Environment, Charles Darwin University, Casuarina, NT 0810, Australia

Corresponding author: Sami Azam (sami.azam@cdu.edu.au)

ABSTRACT Binaural hearing is the ability of the human auditory system to integrate information received from both ears simultaneously. Binaural hearing is fundamental in understanding speech in noisy backgrounds. Any disfunction in one or both ears could cause a disruption in the processing mechanism. Auditory evoked potentials (AEPs) are electrical potentials evoked by externally presented auditory stimuli from any part of the auditory system. A non-invasive technology, electroencephalography (EEG) is used for the monitoring of AEPs. The research aims to identify the best suited electrode positions through correlation analysis and analyse the AEP signals from the selected electrodes in order to detect binaural sensitivity of the human brain. The study evaluates the time-averaged EEG responses of normal hearing subjects to auditory stimuli. The stimuli used for the study are 500 Hz Blackman windowed pure tones, presented in either homophasic (the same phase in both ears) or antiphasic (180-degree phase difference between the two ears) conditions. The study focuses on understanding the effect of phase reversal of auditory stimuli, an under interaural time difference (ITD) cue, on the middle latency response (MLR) region of the AEPs. A correlation analysis was carried out between the eight different locations and as a result, Cz and Pz electrode positions were selected as the best suited positions for further analysis. The selected electrode signals were further processed in the time domain and frequency domain analysis. In the time domain analysis, it was found that Cz electrode for eight subjects out of nine and Pz electrode for seven subjects out of nine, had the larger area under signal curve obtained in the antiphasic condition than in the homophasic signals. Frequency domain analysis showed that the frequency bands 20 to 25Hz and 25 to 30Hz had the most energy when elicited by antiphasic stimuli than by homophasic stimuli. The findings of this study can be further utilised for the detection of binaural processing in a human brain.

INDEX TERMS Auditory evoked potential (AEP), electroencephalogram (EEG), correlation, homophasic, antiphasic, time domain analysis, frequency domain analysis.

I. BACKGROUND

The paired ears can work together for sensing the sound from the outside world with the presence of background noise. The process by which humans can hear and interpret sound with two ears is referred to as binaural hearing. Binaural hearing is the ability of the human auditory system to integrate information received from both ears simultaneously [1]. With binaural hearing, people can perceive where a sound is coming from (sound localization) and choose to focus on one sound even when other background noises are present (sound segregation) [2], [3]. Binaural hearing is essential for understanding speech in noisy backgrounds, commonly referred to as 'the cocktail party effect' [4]–[6]. According to prior research on hearing loss among children, it is noted that any untreated binaural hearing impairments can impede the child's development, in particular verbal cognition skills [7], [8]. People can also suffer from binaural hearing disorders and other hearing impediments in adulthood. Studies have been carried out to understand the relationship of age and hearing problems by performing comparisons between people with normal hearing and people with unilateral or bilateral hearing loss. Most of

The associate editor coordinating the review of this manuscript and approving it for publication was Vincent Chen.

the research indicates that hearing disorders increase with age and that they can affect the quality of life and limit further cognitive development. [9]–[11].

The auditory cortex plays a significant role in hearing. It is a part of the auditory system, which is responsible for performing different functions of hearing [12], [13]. The signals generated from the brain in response to various events can be analysed to study the human processing system. Initial auditory processing occurs in the brainstem and the mesencephalon (midbrain) where responses such as auditory reflexes are co-ordinated, while subsequent stages of processing occur in the auditory cortex of the temporal lobe [14]. Auditory signal processing in the brain can be studied by analysing auditory cortex signals in detail. Event Related Potentials (ERPs) are defined as the brain electrical activity that is triggered by the occurrence of events or stimuli [15]–[17]. Steady State ERPs are evoked continuously during the delivery of the stimulus. They are phase-locked to that stimulus. A non-invasive method of recording such type of electrical potentials could be very useful in detecting abnormalities in sensory pathways and brain disorders related to language and speech [18], [19]. ERPs can be produced from a multitude of sources and represent neural activity from sensory, cognitive or motor events. They form a sequence of deflections or waves, each characterized by different features, of which the latency and amplitude are key factors [20]–[22].

Most of the existing hearing screening methods are unlikely to detect a binaural hearing disorder in isolation. One of the possible methods that can be used in the detection of binaural processing is by analysing brain signals is Electroencephalography (EEG) [23]. This technique measures the scalp potentials at the delivery of auditory stimuli in order to diagnose hearing disorders [24]. The EEG method removes reliance on participant literacy and communication skills and is easier for the participant to perform than the standard psychoacoustic tests, making it highly suitable for children. The EEG can be more difficult to collect than traditional hearing assessments, however if correct stimulus parameters, recording standards and processing techniques are used, this method is both suitable and feasible for binaural sensitivity assessment. The electrical potential generated by large populations of active neurons is recordable on the scalp surface during the EEG measurements. However, the recorded signals are very small in amplitude (ranging from nanovolts to a few microvolts). EEG is a useful technique for clinicians and researchers and is also of utmost importance for testing hearing in cases where a behavioural audiometric assessment is impractical (for example infant hearing screening) [25], [26]. Auditory evoked potentials (AEPs) are recorded from the scalp of the subjects. The wave morphology of the transient wave EPs depend on the strength and type of the stimulus applied, the position on the scalp of the electrode and the response of the subject [27]. The individual evoked potentials have low amplitudes, ranging from 0.5 μV to 10 μV. Since the amplitude of an EP is small compared to the amplitude of spontaneous neural activity, it is difficult to observe an EP in an EEG recording. The target signal (the EP) must be extracted from the "noise" of other spontaneous neural activity [28]. The most commonly used method for EP extraction from other noise signals is the technique of averaging. Since the spontaneous neural activity can be considered as a random process of positive and negative values, the averaging of these values over time will result in near zero values. In order to eliminate the relative noise in measurements, repeated evoked potential sweeps are averaged [29], [30]. Usually, the potentials are measured as the potential difference with a reference electrode. In order to avoid introducing more noise into an AEP signal where the signal to noise ratio (SNR) is naturally low; the generated output requires amplification of at least a factor 10,000 [18]. The configurations used for the electrode placement and the number of electrodes to be placed on the scalp both vary depending on the type of application. The standard configuration is the international 10-20 electrode placement system which prescribes the proportional distance between electrodes relative to the participant's head [31], [32].

While selecting the EEG electrodes for the ERP signal analysis, it is necessary to understand the relationship between signals from electrodes at different locations [33]. The human brain is a very complex structure which consists of numerous neurons that communicate [34]. Recently an area of research is the investigation of the functional connectivity between and within the different regions of the brain in response to different stimuli [33], [35]–[37]. In this research, the connectivity of the different areas of the brain is investigated by analysing the multichannel EEG data acquired for the study of AEPs related to binaural processing. Several studies related to the connectivity of brain regions were found in the literature [37]–[41]. However, few researchers have demonstrated the dependency of electrode locations for the detection of Event Related Potentials [42]. Bonita et al [43] stated that various features and characteristics of EEG data are the indicators of the distinct brain activities occurring in different brain regions. The correlation analysis on the EEG signals from various parts of the brain obtained through different electrodes mainly indicates that a high correlation between the signals shows a high interdependency which, in turn, relates to similar brain activity [44]. Some researchers found that while brain activity within local regions might be dependent, there were non-dependency between the global non-identical regions [45]. A correlation analysis of the EEG signals acquired for the AEP study is done to determine what relationships exist between ERP signals from electrodes on different regions of the scalp, and to investigate whether this could provide any further information in the study of binaural hearing in human brain [36].

Considering the brain anatomy, distinct functions are carried out by the different brain areas. Figure 1 depicts the brain lobes. The frontal lobe mainly stands for the intentional and motivational centres and is close to sources of emotional impulses [46]. The sensory and motor functions are dealt with by different cortical locations, of which Cz is the
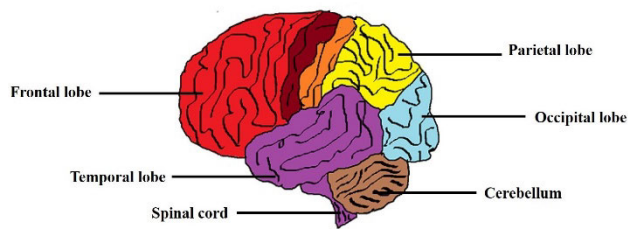
FIGURE 1. Lobes of the brain - Anatomy.

centre [36], [47]. The parietal lobe and nearby areas contribute to the differentiation and perception functions [13]. The temporal and occipital lobes correspond to the emotional processing, memory functions and primary visual actions respectively [36].

Since the ERP signals from the brain are time locked spontaneous events corresponding to sensory, motor or cognitive stimuli, they can be analysed in the time domain, the frequency domain or a combination of both for better understanding. Auditory Evoked Potentials (AEPs) are commonly analysed by averaging in the time domain. The waveform of the averaged scalp is commonly used in research. D J Strauss et al [48] have concluded that ABR time-scale representations are suitable for analysing binaural interaction in human brain. In addition, the spectral power and entropy features have been extracted from the recorded AEPs and used for the classification of conductive and sensorineural hearing loss [49]. This study also provided insight in the feasibility of fewer electrode channels to detect different hearing loss using a feature band-score index. A Kumar et al [50] combined different time-domain and frequency domain parameters to identify the best way to distinguish the awake state from the anaesthetized state. The amplitudes and latencies of the MLR signal peaks were used in their study. In a study by S A Hillyard et al [51], peak amplitudes and latencies of AEPs were analysed for subjects who either selectively listened to the stimuli in one ear or ignored them. They found a potential significant difference in the amplitudes between the conditions. Similarly, gender based differences in all the latencies and the inter peak latency of the BAEP were studied for a healthy elderly population [52]. The conclusion was that the gender-based difference in the AEP were not statistically significant. In addition to time domain analysis, the relative wavelet energies in specific frequency bands of AEPs have also been studied. It was observed that the continuous time wavelet entropy (CTWE) can be used as an alternative method to analyse AEPS [53]. Frequency domain analysis for the AEPs are also described in literature. Spectral analysis to identify the prominent frequencies present in an AEP helps the researcher to get insight in the characteristics of the responses of subjects under study and helps in selecting the best filter bands. Analysis of AEP signals with FFT to investigate hearing ability was done by M Paulraj *et al.* [54]. Features extracted with FFT were used for artificial intelligence algorithms. R A Dobie et al [55], presented a coherence analysis for the evoked potentials generated in response to clicks and tones, as an alternative to common spectral analysis in the frequency domain. In different studies [56]–[58], frequency domain analysis of the AEPs was carried out in order to identify the detectable features and characteristics relevant to the stimuli provided. There is a wide range of literature related to the Audiometric EEG. There is a lack of relevant literature, however, regarding binaural hearing testing stimuli for the Audiometric EEG. This indicates that an avenue for future studies is available and a contribution to the existing body of knowledge can be made.

Our work aims to understand the effect on AEPs while presenting the stimuli in homophasic and antiphasic conditions, which may be an indicative for binaural sensitivity. However, for the ERP measurements, the requirement to use a large number of electrodes is not essential. To be fast and affordable in a clinical setting, the drawback of using a large number of electrodes [59], [60] might make the entire system inefficient in terms of cost and time. The purpose of this study is to analyse which EEG electrodes are most useful in order to obtain high-quality information related the auditory processing. The optimal selection of electrode locations for the ERP data acquisition depends on the different functions of the brain lobes.

In this study, we try to find the best-suited electrode locations by investigating the connectivity of EEG signals recorded from different electrode positions in multichannel EEG measurements. This is investigated by the correlation analysis technique [42]. The signals from the selected electrode positions were then analysed to detect binaural sensitivity in the brain from the AEP waves corresponding to the application of homophasic and antiphasic stimuli [61]. The study involves the use of active electrode cap which significantly reduces the electrode montage and subject preparation time [62]. Besides, the active electrode increases the SNR and reduces the influence from unwanted noise in the EEG data acquisition including the eye movements, active and passive head movements, cable movement artefacts etc [62], [63].

II. METHODOLOGY

The study was carried out at Charles Darwin University, Australia. The experimental protocols as explained in H18014 – Detecting Binaural Processing in the Audiometric EEG were approved by the Humans Ethics Committee of the University. A written consent that indicates the willingness of volunteer to take part in the different hearing test including the EEG measurement were collected before the conduction of the experiment. A plain language statement (PLS) with the details of the study is also explained for the overview of the experiment process and a questionnaire was completed by each subject to ensure a healthy otological history.

A. EXPERIMENTAL FLOW

The experiments were conducted in a sound-proof room in order to minimise background noise [64]. The participants
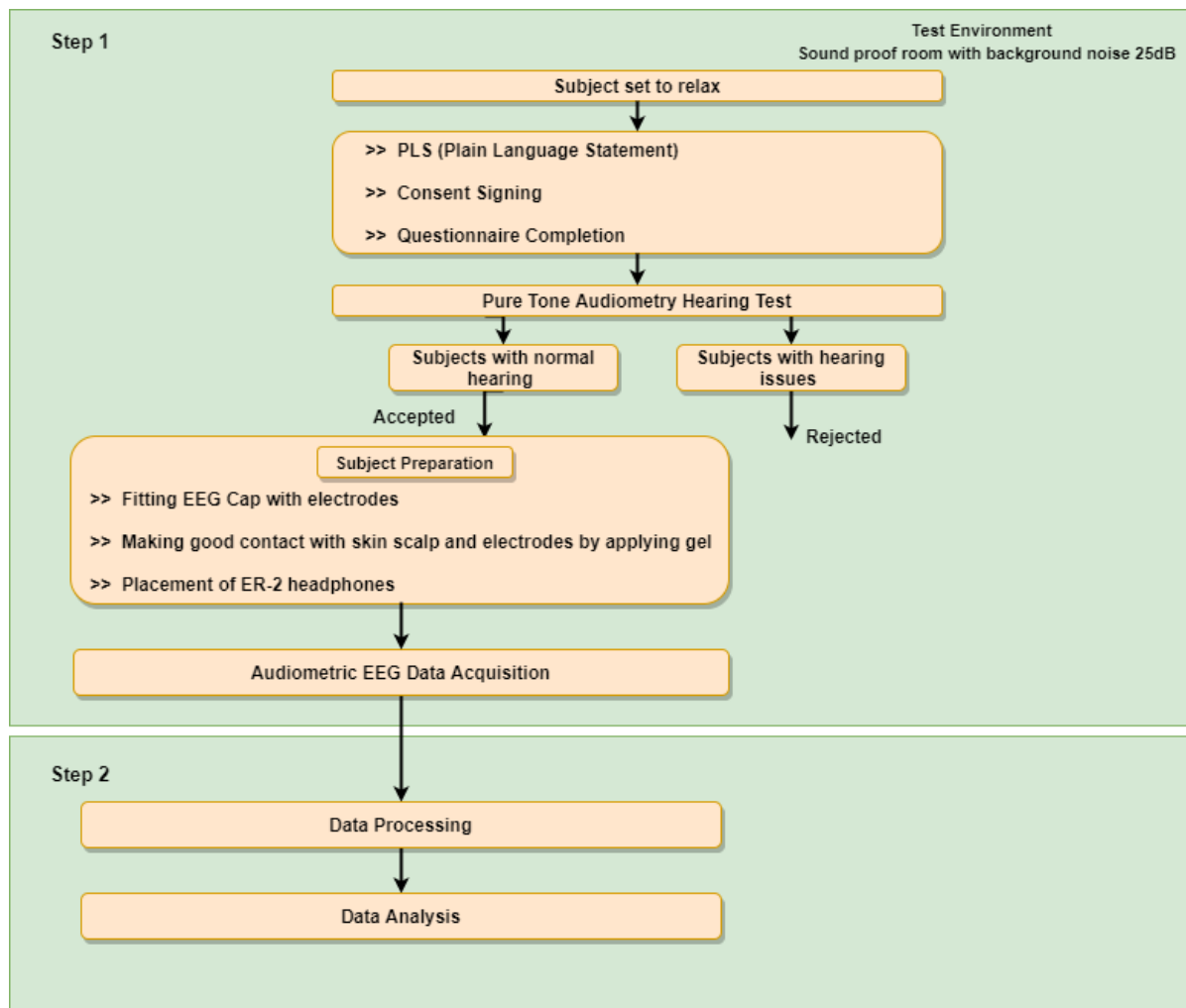
FIGURE 2. Experimental Flow.

were instructed to sit and relax for five minutes before the beginning of the test. Figure 2 depicts the sequence from the start of the experiment till the analysis of the data. As per the protocol of approved ethics, a Plain Language Statement (PLS) was read to the participants before the start of every test to ensure that they were aware of the details of the measurement procedure and any risks involved and participant need to sign a consent form. The volunteers were then given a questionnaire to obtain their otological history. Next a hearing threshold test was performed [65]. The responses to the questionnaire and the results of the hearing test were analysed immediately to screen out ineligible participants. Once the suitable subjects were selected after screening, they were prepared for the auditory EEG test [66]. The subject preparation includes the application of the gel, the placement of the EEG cap with electrodes at the points of interest according to the international 10-20 system [67], and the placement of earphones. All the hardware and software were then connected properly. Care was taken to avoid artefacts that can affect the reliability of the test. After ensuring the

subject was not experiencing any discomfort, the stimuli were delivered to the earphones and the EEG data were acquired. The recorded data were stored. Data processing and analysis of the captured EEG data was carried out afterwards.

B. EXPERIMENTAL SETUP AND HARDWARE

Figure 3 illustrates the set up used for EEG data acquisition. The experimental set up utilizes two separate computers, one for the delivery of the stimulus and the other to capture the EEG data. In EEG data acquisition, the auditory stimuli are presented to the ER.2 insert earphones via an external sound card (Creative Sound Blaster Omni Surround 5.1). The ER.2 research earphones used for the audio stimulus delivery were calibrated at 60dB Sound Pressure Level (SPL) before the start of every hearing test. This ensures that the volume of the stimuli transferred to the subject's earphone is correct. ER.2 earphones are selected for the study minimise electromagnetic coupling issues [68]. The stimuli along with the trigger pulses were sent to the bio amplifier, 'g.USBAMP'
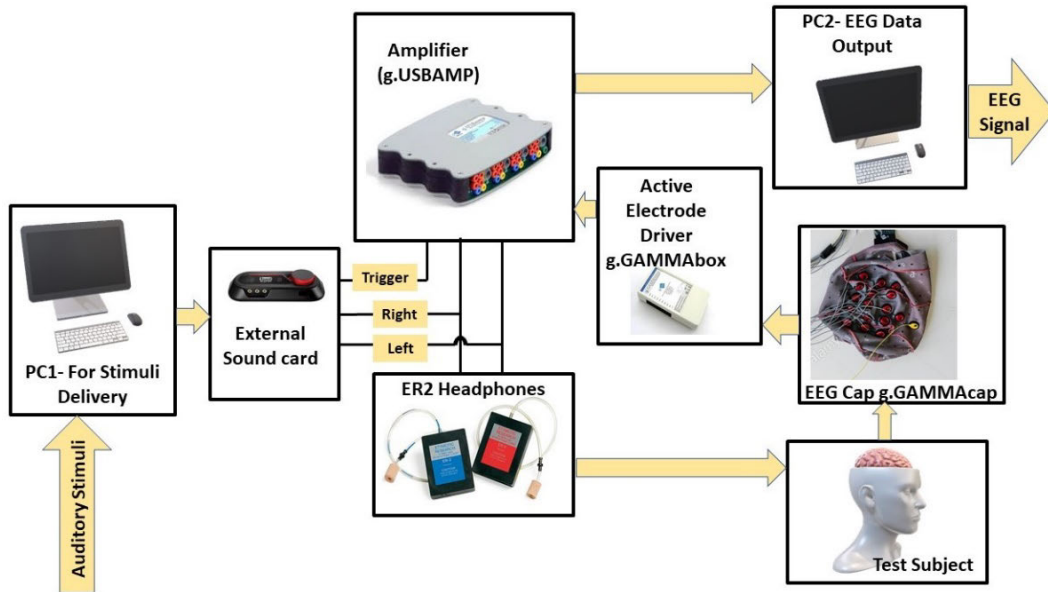
FIGURE 3. Data Acquisition System.

through specially designed audio cables (to achieve the input voltage requirements of the amplifier). The trigger signal is synchronised with the audio stimulus to aid in epoch detection. More specifically, the trigger signal identifies the actual point in time each stimulus is delivered which is then used to extract the correct AEP data. The G.Tec USB biosignal amplifier (Guger Technologies OG, Austria) has been used. It has a sampling rate of 19.2 kHz. The amplifier has four individual blocks with four separate channels each. All four blocks have a ground as well as a reference input to assist in the elimination of interference from other channels. The amplifier can record 16 channels simultaneously with a 24-bit resolution. G.Tec g.GAMMASYS active electrode system was used for the multichannel EEG audiometric data recording from eight different locations. This enables the connection of active EEG electrodes from the G.Tec g.GAMMAcap on the head of the subject to the G.Tec USB biosignal amplifier via the G.Tec g.GAMMAbox. The active electrode cap system makes subject preparation easier and reduces the sensitivity to different artefacts due to the inbuilt preamplifier of 1-10 gain which ensures more reliable data recording [62]. The EEG data acquired from the captured PC2 were then processed and analysed.

C. PARTICIPANTS

Nine normal hearing subjects (five males and four females) with a mean age of 26 years were selected in the initial study.

A pure tone audiometry hearing test was carried out to detect the hearing threshold levels of participants at different frequencies in accordance with the relevant Australian Standards and determine whether these were acceptable. The Australian Standards for the hearing tests include:
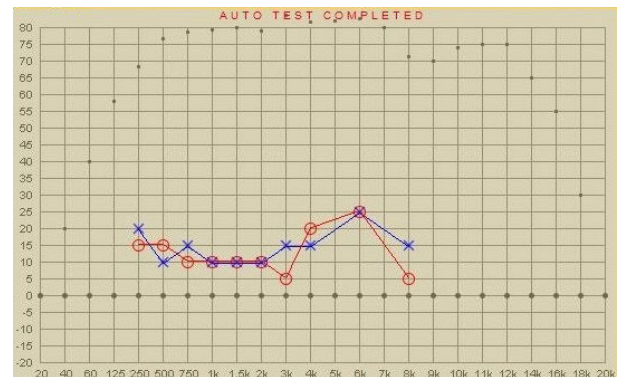

FIGURE 4. Sample audiogram.

➢ AS/NZS 1269.4:2014 – Electroacoustics Audiological Equipment (Part 1: Pure-Tone Audiometers).
➢ AS IEC 60645-1:2000 – Occupational Noise Management (Part 4: Auditory Assessment).

The Digital Audiometer Professional (DAP) software was used for the pure tone audiometry hearing test. A series of pure tones were presented to the subject through insert (air conduction) earphones, first to the left ear, then to the right. The subject had to press the 'SPACE' bar as soon as they heard the sound. This test takes about 5-10 minutes per ear. The DAP software can test the frequency range between 0 and 22,000 Hz with an amplitude range of -20 dB to 100 dB for each frequency. The conventional range of frequencies for audiometric testing is 500 Hz to 8 kHz. However, this research tested the frequency range from 125 Hz to 8 kHz as this may be relevant for binaural hearing. The background noise level was maintained at 25 dB, the acceptable level for audiometric testing [64]. Figures 4 and 5 show two randomly
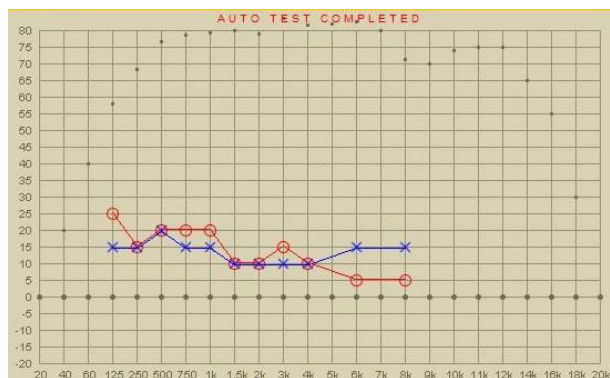
FIGURE 6. Subject with electrodes for data acquisition.

selected sample audiograms for the subjects who underwent the hearing test. The blue and red colour in audiogram represent the left and right ear responses respectively. All the selected subjects had normal audiograms with the threshold value of 20dB hearing level (HL) for the frequency range 125Hz to 8KHz.

D. SUBJECT PREPARATION

The subject preparation process includes the fitting of the electrodes and the electrode cap, verbal instructions regarding experiment conduction and side effects, as well as lowering of the electrode impedance and artefact prevention. Participants were asked to sit relaxed in a soundproof laboratory and were fitted with an appropriate head cap according to their head measurements. The g.GAMMA cap used for the experiment enables the placement of scalp electrodes, as per the international 10-20 system. The use of active electrodes significantly improves the signal to noise ratio (SNR), even without the abrasive impedance minimization and additional cleaning of
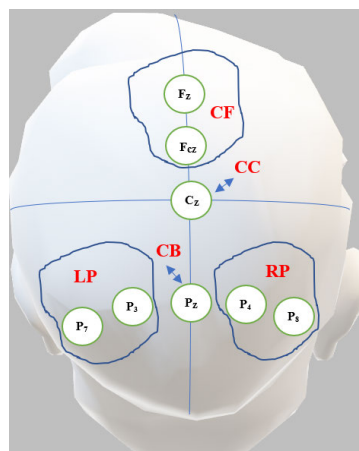

FIGURE 7. Graphical representation of the arrangements of electrodes for EEG measurement.

the skin. This reduces the duration of subject preparation [69]. The active electrodes minimize the artefacts caused by movements and electromagnetic interference. Figure 6 depicts the set up with a subject for data acquisition.

E. ELECTRODE PLACEMENT

In this study the brain regions were divided into five areas for the correlation information: the central front (CF), central cortical (CC), central back (CB), right parietal (RP) and left parietal (LP) regions. The electrode sites chosen for the AEP recording with in these areas under study are in Table 1 [37], [70]. Figure 7 depicts the arrangement of electrodes and their regions for the EEG reading. For these measurements, the reference electrode was placed on the left earlobe and the ground electrode was placed in the lower position (FPz according to 10-20 electrode placement) on the forehead [71], [72].

TABLE 1. Regions and corresponding channels used in the EEG measurement.

Region/Area	Channels
Central Front (CF)	Fz, FCz
Central Cortical (CC)	Cz
Central Back (CB)	Pz
Right Parietal (RP)	P4, P8
Left Parietal (LP)	P3, P7

The selection of these eight different electrode positions for the EEG measurement has taken into consideration the information obtained from the literature describing the location-related functionalities of the brain [73], [74]. Different areas of the brain have different functions. The CF area contains the electrode positions Fz and FCz located near intentional and motivational centres. The CC area which includes the cortex Cz location deals with sensory and motor functions.

Besides to follow the method prescribed in [60] for maintaining symmetry, the electrode position Pz was selected for the CB area. Pz will be symmetrically opposite to that of Fz in the CF area. Similarly, symmetrical electrode positions were chosen on both the left and the right hemispheres, P4 and P8 in the RP region and P3 and P7 in the LP region [75]. This will remove the bias for a single hemisphere, which was indicated as a serious problem in several studies [76], [77]. Locations P3, P4, Pz, P7 and P8 relate to perception and differentiation functions. The locations Fz, FCz, Cz and Pz electrode positions are in the midline of the brain.

Among these, the midline electrode positions Fz, the frontal lobe, Cz, the central region, and Pz, the parietal lobe, have been used for different AEP studies to provide an insight to select the electrode locations with respect to the previous studies. A cortical AEP study was conducted by considering the Fz and Cz locations which are common and where the maximal amplitudes for AEP components are achieved [78]. A recent study, recording EEG from non-human primates, proposes a new head holding system design with the positions comparable to human electrode placements for auditory stimuli which corresponds to the electrode selection of the current research [79]. B I Turetsky et al [80] developed a model to relate the reliability of AEP wave form to signal power, noise power, SNR using the Fz, Cz, and Pz electrode sites. These sites were also used by W T Roth et al [81] who designed for the parameters of temporal recovery of human AEPs. A number of other researchers used the same locations. The effects of ethanol and meperidine on AEPs to stimuli having different intensities [82] and the effect of contralateral masking on cortical AEPs at different masking intensities [83] were also investigated using Fz, Cz and Pz electrode locations as the major sites [82].

The majority of studies with auditory stimuli for analysing the binaural interactions in the human brain focus on the early auditory response generated from the auditory nerve, the cochlear nucleus, lemniscus lateralis and the inferior colliculus [18], [84]. The cortical response to auditory stimuli has also been studied but there is scope for more studies regarding auditory responses generated from the cortex to binaural stimuli. As explained, the regions and the corresponding electrode sites considered most suitable for acquiring an AEP response to these stimuli were included for improving our understanding of binaural interactions in the human brain.

F. AUDITORY STIMULI

The stimuli used in the study were Blackmann windowed pure tones with a frequency of 500Hz. Blackman windowing ensures a smooth acoustic transition between the silence and the start or the end of the stimulus and reduces spectral splatter of the signal [18]. The stimulus was 218 ms in duration, generated in MATLAB R2017b with the signal time of 18 ms, a silence time of 200 ms and was sampled at 19.2KHz. The generated stimuli are illustrated in Figure 8. The stimuli were presented in a predefined sequence.
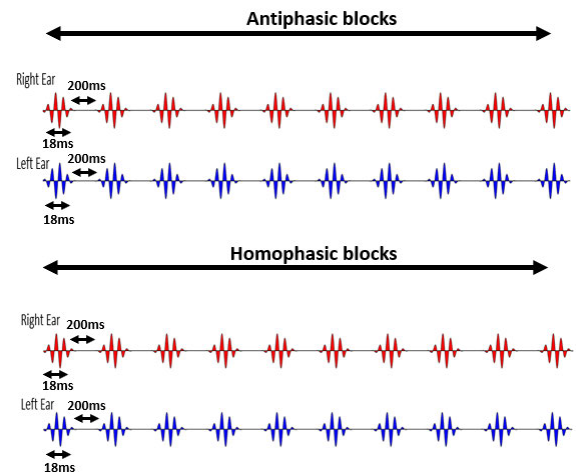

FIGURE 8. Auditory Stimuli.

The stimuli were presented in blocks of 10 antiphasic stimuli followed by 10 homophasic stimuli. Thus, a total of 1000 trials was carried out, resulting in generation of 500 antiphasic and 500 homophasic ERPs. The total time for 1000 trials was 3.37 minutes. According to literature [85]–[87], on average healthy adults have an attention span in the range of 10 to 20 minutes. Hence the risk of the occurrence of hearing fatigue and adaptation during the test period is limited by the relatively short total time for the experimental trial. Subjects were asked to relax before the experiment in order to ensure quality data acquisition. The stimuli were delivered to the earphones at 60 dB sound pressure level. The stimuli were developed using a pure tone sinusoidal signal and its opposite Spi signal. The equation for generating the Spi and So signals were as follows: -

$$So = (1 * \sin(2 * pi * f * T)). * blackman(length(T))';$$
$$Spi = -((1 * \sin(2 * pi * f * T)). * blackman(length(T))');$$

where f is the frequency and T is the Time_vector.

III. ANALYSIS
A. SIGNAL PROCESSING AND ANALYSIS

After the data acquisition process was completed, the data processing and analysis were carried out offline. Figure 9 illustrates the workflow followed for data processing and analysis. The data were imported as an array into MATLAB. This contained the data of the captured EEG channels, the trigger channels and the stimulus channels. Further processing of signals was carried out in MATLAB R2017b using the EEGLAB v2019.1 toolbox. The sampling rate for EEG data acquisition is 19.2 kHz and produces a Nyquist frequency at over 8 kHz which is much higher than required for analysing the frequency ranges in the human AEP. So, in the pre-processing stage, the EEG data were down sampled to 2048 Hz [88] using the EEGLAB function 'pop_resample' which in turn uses the MATLAB 'resample' function. This provides a Nyquist frequency of 1024 Hz which is
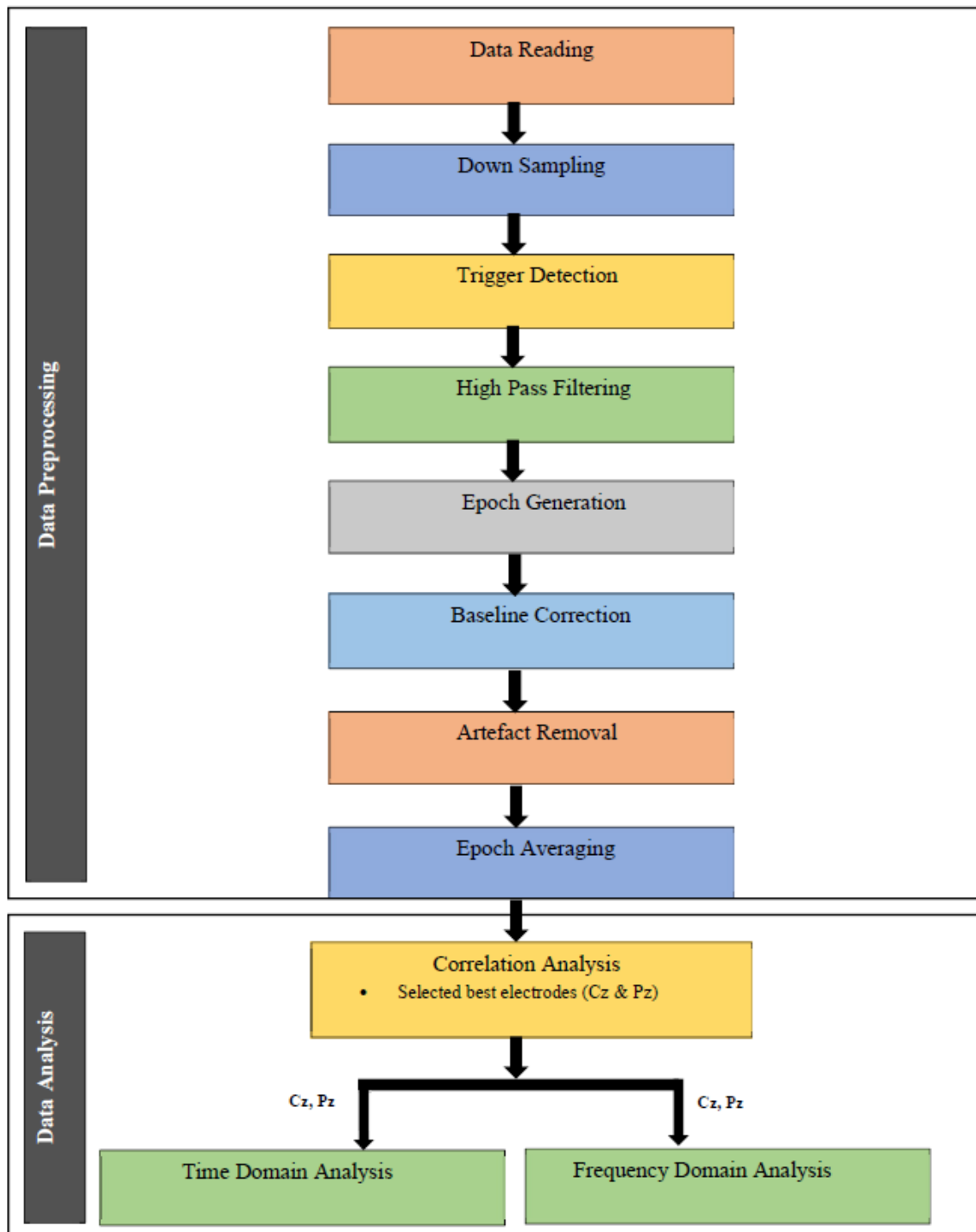
FIGURE 9. Data Processing and Analysis.

still considerably higher than the frequency of interest. The process of down sampling ensures that the filtering process in the pre-processing stage is computationally efficient as well as improving the ability of roll-off of the filters [62], [89]. The next step in data pre-processing was to extract the accurate trigger times by removing the triggers before 1s and by checking whether 1000 triggers were found in total. The detection of the triggers was done by checking the time between two triggers (it should be TRIAL_DURATION (0.218s) and if a lesser time delay was found, the corresponding trigger was rejected. The trigger channel data captured by the amplifier were used for the synchronized averaging

FIGURE 10. Trigger detection process.

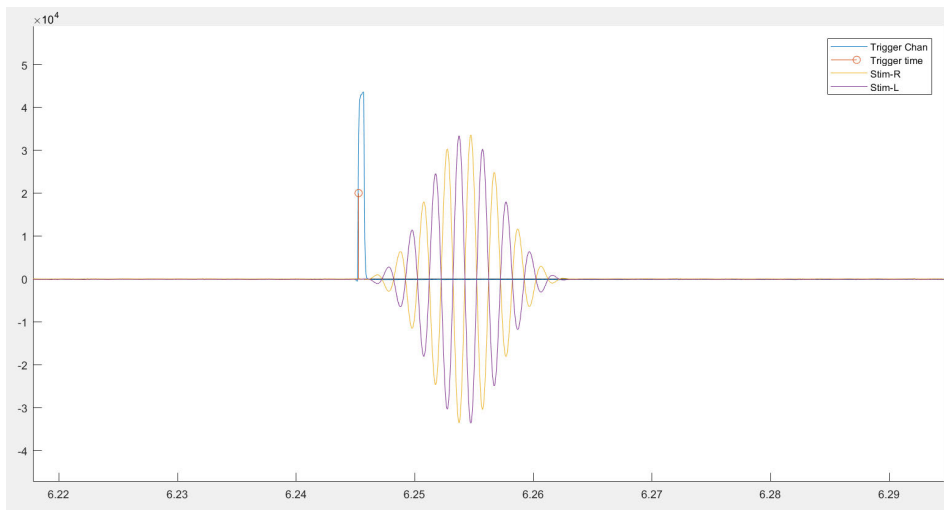process. As in Figure 10, the actual triggers were detected by analysing the right stimuli (Stim-R) and left stimuli (Stim-L) together with the trigger timing. In figure 10, it is clearly seen the triggers at the start of each stimulus were detected accurately and incorrect triggers were eliminated.

Once the triggers were detected, artefacts and noise were removed to obtain clear evoked responses for further processing and analysis. A high pass filter with a cut-off frequency 1Hz was then applied to the data to attenuate slow drift noise and DC components from the signal [90], [91]. The filtering process will clean the data for better AEP analysis.

The next stage of data processing involves the epoch generation. Using the valid trigger signal and the phase of the stimuli in both left and right channels, the responses to homophasic and antiphasic signals were located. The evoked potentials were then analysed in epochs (pre-defined short duration of time of interest) [84], [92]. The start and duration of the epoch were determined using the trigger signal which was delivered synchronously with the stimulus and the duration of the signal and the silence between the signals [93]. For this study, the epoch used is the signal from 20ms to 218ms after the trigger signal which includes the entire Middle Latency Response (MLR) to the given stimuli. A baseline correction was done by subtracting the mean value for each trial. Epochs with significant artefacts were excluded by rejecting epochs that had an absolute amplitude of 150 μV or more [94], [95]. The remaining epochs were averaged for the best reflection of the shape of AEP wave, maximum noise reduction and improved Signal to Noise Ratio (SNR) [96].

The data pre-processing, including the epoch averaging, was carried out separately for each of the eight electrode locations. Once the pre-processing stage had been completed, the averaged AEP signals were further analysed. The analysis of the AEP data mainly focused on binaural processing in the brain. A correlation analysis was carried out to find the best electrode positions for the AEP data acquisition. Once the

electrode positions were selected, the signals were further analysed in both the time and the frequency domain to investigate the response to homophasic and antiphasic signals which can be indicative of binaural processing of the brain.

B. OPTIMAL CHANNEL SELECTION WITH CORRELATION ANALYSIS

A correlation analysis was carried out to determine the best electrode positions for the analysis of AEPs. As shown in Figure 7, different regions of the brain were selected, and the corresponding EEG channels were used for correlation analysis. During the correlation analysis, the relation for electrode positions in the different regions of the brain from the ERP signals was analysed using the Pearson correlation coefficient. The Pearson correlation coefficient of two random variables is a measure of their linear dependence. If each variable has N scalar observations, the correlation coefficient is as follows:

$$\rho(A, B) = \frac{1}{(N-1)} \sum_{i=1}^{N} \left(\overline{\frac{A_i - \mu_A}{\sigma_A}}\right) \left(\overline{\frac{B_i - \mu_B}{\sigma_B}}\right) \quad (1)$$

where A and B are the two variables corresponding to the two electrode positions under analysis. The μ_A and σ_A values are the mean and the standard deviation of A and the μ_B and σ_B are the mean and standard deviation of B respectively. Using the coefficients, correlation plots were obtained for both the homophasic and antiphasic data. Figure 11 and 12 depict the correlation plots for a representative subject for homophasic and antiphasic stimuli. The aim of the correlation study was to identify best electrode position for audiometric EEG measurements. It can be seen that the intercorrelational maps for homophasic and antiphasic stimuli for the selected subject are same.

Once the initial correlation coefficients were determined for individual electrode positions the correlation between
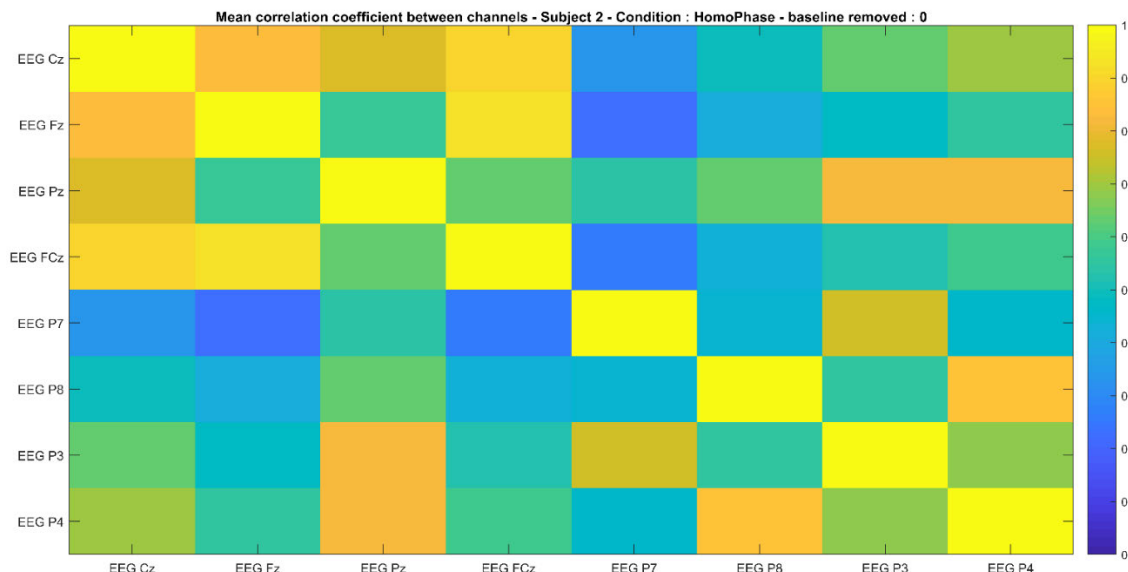
FIGURE 11. Correlation between channels for a representative subject is shown for the Homophasic stimulus.
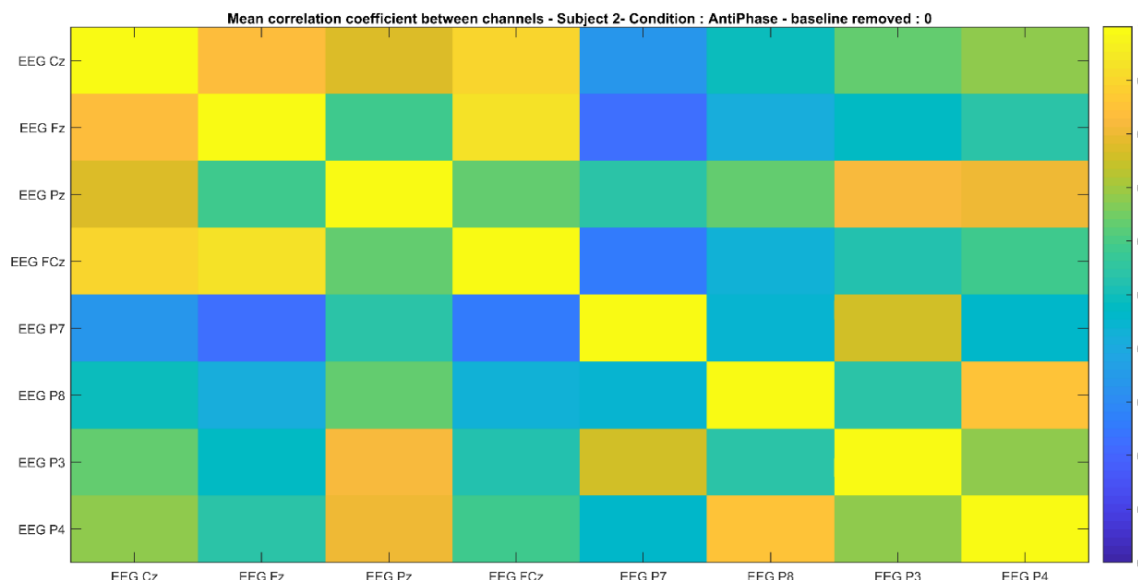

FIGURE 12. Correlation between channels for a representative subject is shown for Antiphase stimulus.

the different regions was carried out. Afterwards, the average cross-correlations for specific regions were found. For instance, the central front region was analysed for the connectivity with the right parietal, left parietal, central back and central cortical regions. Similarly, the connectivity of the right parietal, left parietal, central back and central cortical regions with each other were also analysed and plotted. To perform the average cross-correlation analysis, the mean values of the individual electrode's coefficients were used with respect to the area under analysis. A rank table of the obtained results was generated by counting the

number of more correlated regions and the best electrode regions for the study of binaural processing were determined. The P-value was calculated to determine whether the results are statistically significant [42], [97]. The colour yellow stands for highly correlated regions in the correlation maps shown in Figure 11 and 12. As the colour indication turns from yellow to blue, the correlation decreases. For example, from figure 11, we can see that Pz, Fz, Cz and FCz have a strong correlation to each other, indicating strong connectivity lying in the midline of the brain. Similarly, P7and P3 as well as P8 and P4 shows a strong correlation to Pz since
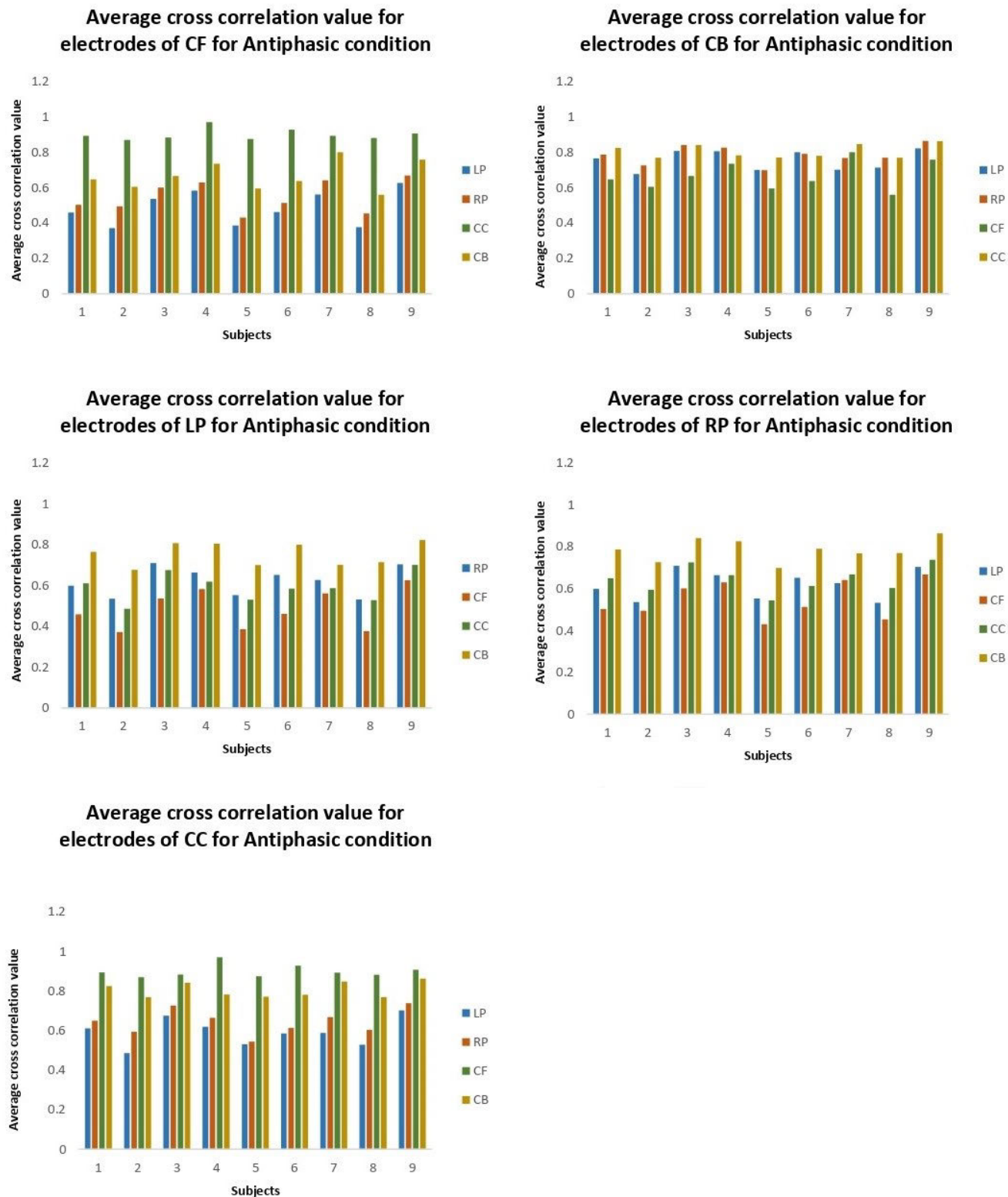
FIGURE 13. Average cross correlation values for nine subjects between different regions in antiphasic condition (CF - Central Front, CC - Central Cortical, CB - Central Back, RP - Right Parietal, LP - Left Parietal).
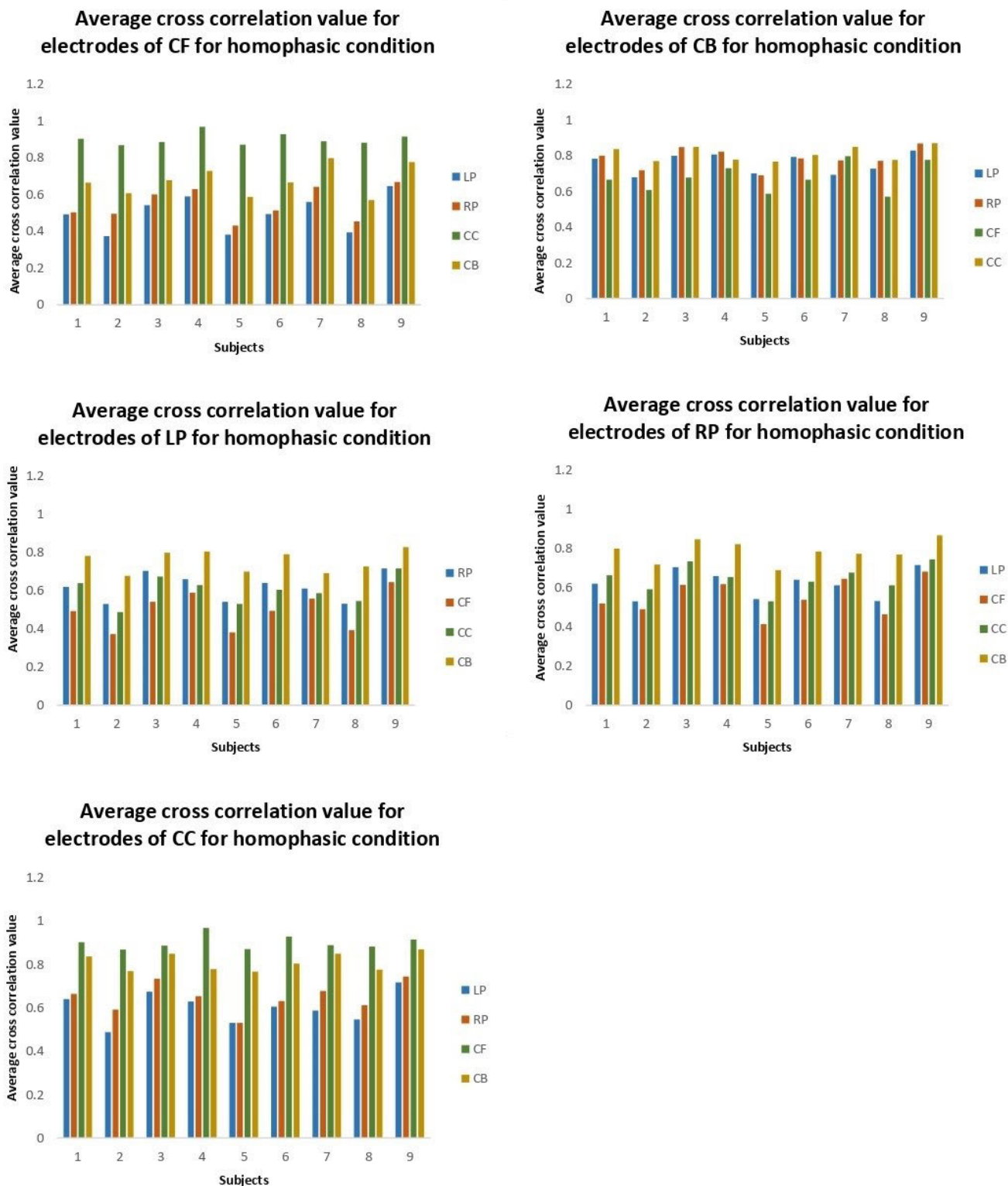
FIGURE 14. Average cross correlation values for nine subjects between different regions in homophasic condition (CF - Central Front, CC - Central Cortical, CB - Central Back, RP - Right Parietal, LP - Left Parietal).

they all are the locations in the parietal lobe. However, there was less connectivity between the right parietal (RP) and the left parietal (LP) locations, as shown by the blue colour

indication. Also, the electrodes in the frontal lobe, Fz and FCz, are having a strong connection to the Cz location but not to more distant electrodes [98]. This reflects the functional

TABLE 2. The rank table for the Antiphase condition (CF - Central Front, CC - Central Cortical, CB - Central Back, RP - Right Parietal, LP - Left Parietal).

With CC			With CB			With LP		
Rank	Region	Correlation	Rank	Region	Correlation	Rank	Region	Correlation
1	CF	0.8989	1	CC	0.8040	1	CB	0.7524
2	CB	0.8040	2	RP	0.7836	2	RP	0.6157
3	RP	0.6414	3	LP	0.7524	3	CC	0.5875
4	LP	0.5875	4	CF	0.6625	4	CF	0.4759
With RP			With CF			Rank Table_ Antiphasic Condition		
Rank	Region	Correlation	Rank	Region	Correlation			
1	CB	0.7836	1	CC	0.8989			
2	CC	0.6414	2	CB	0.6625			
3	LP	0.6157	3	RP	0.5418			
4	CF	0.5418	4	LP	0.4759			

TABLE 3. The rank table for the Homophasic condition (CF - Central Front, CC - Central Cortical, CB - Central Back, RP - Right Parietal, LP - Left Parietal).

With CC			With CB			With LP		
Rank	Region	Correlation	Rank	Region	Correlation	Rank	Region	Correlation
1	CF	0.9001	1	CC	0.8096	1	CB	0.7541
2	CB	0.8096	2	RP	0.7836	2	RP	0.6139
3	RP	0.6453	3	LP	0.7541	3	CC	0.5977
4	LP	0.5977	4	CF	0.6699	4	CF	0.4878
With RP			With CF			Rank Table_ Homophasic Condition		
Rank	Region	Correlation	Rank	Region	Correlation			
1	CB	0.7836	1	CC	0.9001			
2	CC	0.6453	2	CB	0.6699			
3	LP	0.6139	3	RP	0.5418			
4	CF	0.5475	4	LP	0.4878			

connectivity of brain regions. Moreover, from the plots, it was clear that all these electrode positions had a strong relation to the Cz and Pz locations.

After the cross-correlation analysis between the electrode positions, an average of the obtained coefficients was plotted to investigate the relationship between the different regions of the brain under study. In this process, each region is correlated to the remaining regions. The plots in Figure 13 and Figure 14 depict the region-wise correlation analysis for all nine subjects in antiphasic and homophasic conditions respectively.

The correlation plots for the region-wise analysis provide a clear illustration of the relation between the regions of the brain while measuring the ERPs. For example, in Figure 13 (a), the average cross-correlation between the regions CC, CB, RP and LP with CF region is shown. As shown in figure 13, the frontal lobe is more related to the central cortical region and central back. However, the

correlation coefficient was less than 0.5 between CF and the left and right parietal regions. This illustrates the relationship between the electrodes in different areas of the brain to the remaining regions under study. A similar relation can be seen for the homophasic condition. The calculated mean values for the region-wise correlation were also tabulated to generate a rank table. Table 2 and Table 3 show the rank order of the regions with electrodes for the ERP data acquisition based on the correlation analysis.

Regions with rank 1 in Table 2 and Table have the highest correlation values. It can be seen that the regions CC and CB had rank 1 most often. Hence for the further analysis, we are considering the electrodes in CC and CB region with the Cz and Pz channel locations since they highly correlate with all other regions under study.

The next step was the calculation of the P-value calculation to analyse the statistical significance of the results for the different channels. Figure 15 and Figure 16 shows a plot of the
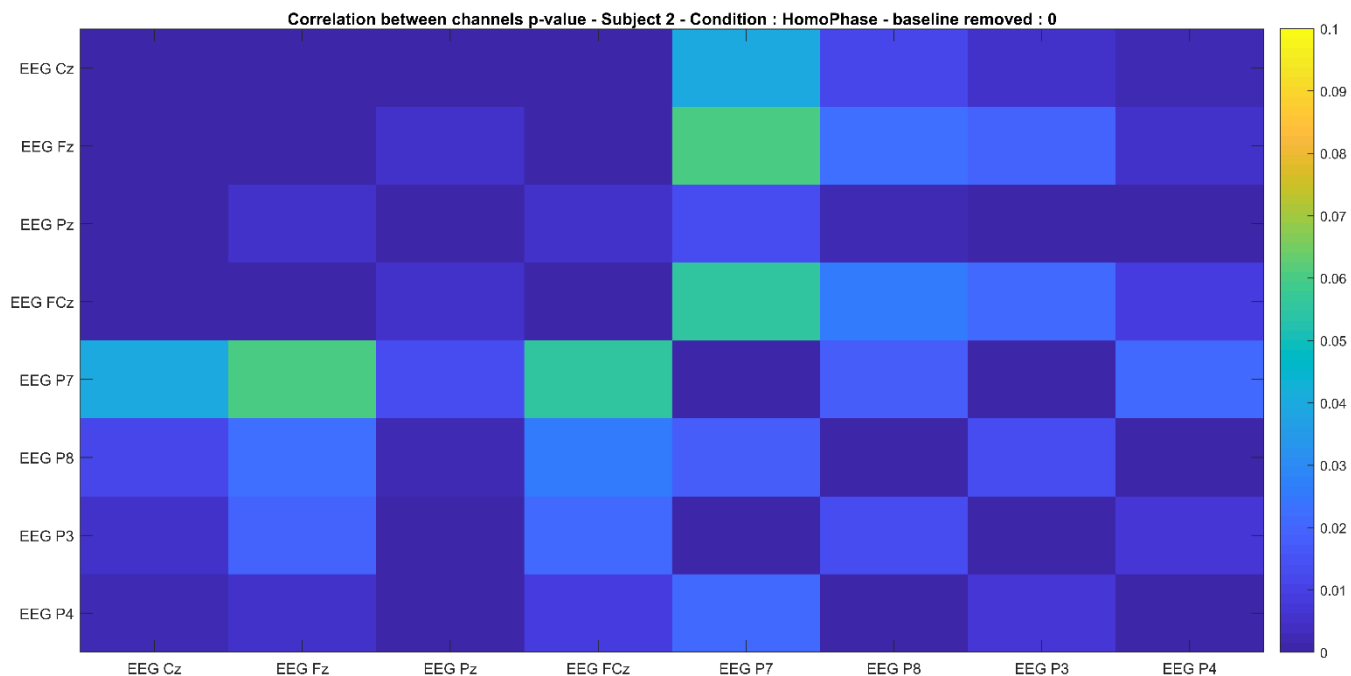
FIGURE 15. Correlation p-value Homophasic condition.
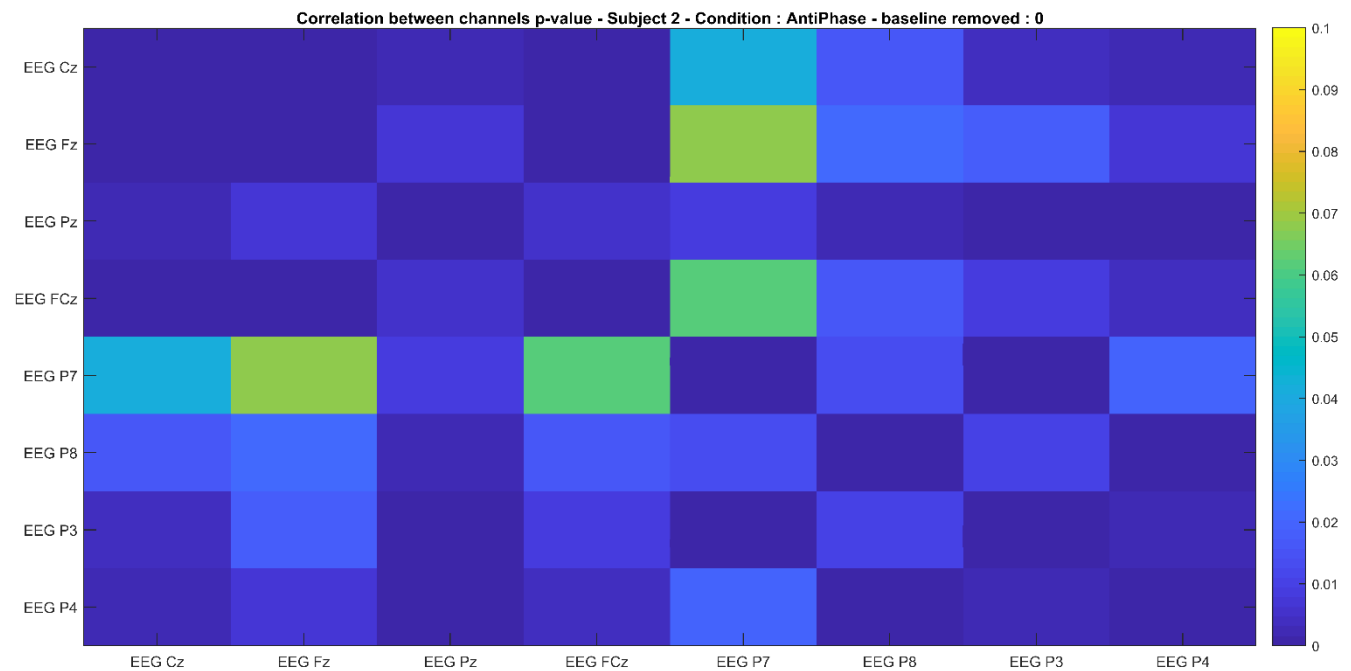
FIGURE 16. Correlation p-value Antiphase condition.

P-values for one subject for both homophasic and antiphasic stimuli. The dark blue colour indicates that $0 > p < 0.01$ for the electrodes in the central front and central back lobes which reveals the statistical significance of the acquired data. The correlation shows an inverse relationship with the distance on the scalp [42].

To study the relationship between the homophasic and antiphasic stimuli responses a further correlation analysis was done, see Figure 17. The blue colour in the Figure indicates that the values are close to 0. This shows that the homophasic and antiphasic signals are weakly correlated and that there exists a significant difference between the observed responses
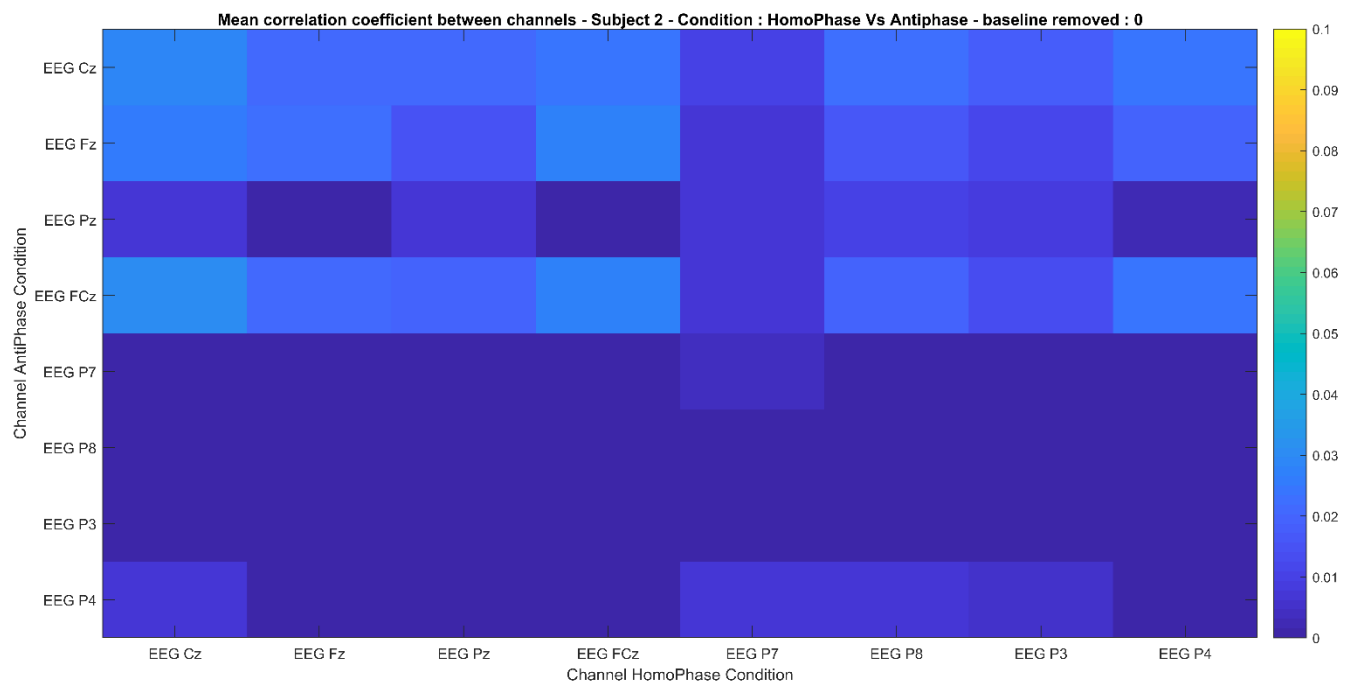
FIGURE 17. Correlation Antiphase vs Homophasic. The difference between the antiphase and homophasic signal correlations at all channels for a representative subject is shown.

to the antiphasic and homophasic signals. This supports the fact that the phase difference can serve as a binaural cue which is useful in the analysis of the binaural hearing in the brain [99]–[101]. Applying the technique of correlation analysis, we were able to identify the optimal EEG electrode location to be utilized in audiometric EEG in order to distinguish the EEG responses to different signals for the study of binaural hearing [102].

Since the channels Cz and Pz are highly correlated to all the other electrodes in the different regions of the brain, further analysis was carried out on these channels. Moreover, after the correlation analysis, it is evident that the channels Cz and Pz can represent the most significant data required for the AEP analysis.

C. TIME DOMAIN ANALYSIS

Based on the correlation results, the Cz and Pz channels were chosen for further data analysis. Time-domain analysis of the Cz and Pz EEG channels was carried out to investigate evidence of binaural processing. In the time domain analysis, the AEPs for the homophasic and antiphase conditions for the selected channels were plotted with a 95% confidence interval for each subject. Along with, the area under the time domain, the ERPs for both homophasic and antiphasic conditions were calculated and analysed. The time-domain representation of the averaged homophasic and antiphasic ERPs elicited by the 500Hz stimulus for Cz and Pz channels of

a randomly selected subject are shown in Figures 18 and 19 respectively.

The red signal in Figure 18 and 19 corresponds to the antiphasic condition and the green signal to the homophasic condition. The averaged time-domain signals were plotted within the 95% confidence interval for the time interval 0ms to 218ms. The area under the squared ERP for both conditions for the time interval 20ms to 218ms was computed and tabulated as in Table 5. In Table 5, Area_out stands for antiphasic and Area_in stands for homophasic respectively. The trapezoidal rule was used for the area calculation under the ERP curve and it was implemented with the Matlab function trapz(y).

Table 4 provides the area values for the time domain plots of the homophasic and antiphasic signals for the Cz and Pz channels. The difference in the area for both conditions was also calculated for all nine subjects. It can be seen from Table 4 that for the channel Cz, for all subjects except subject 8 the area for the antiphasic condition was larger than the area for the homophasic condition. Hence for the Cz location, 90% of subjects under analysis, have a higher underlying area for antiphasic signals compared to the homophasic signals. For the Pz channel, also shown in Table 4, 7 out of 9 subjects, or approximately 80%, had an area under the curve which was greater for anti-phase stimulus than for the in-phase stimulus. The larger area for the antiphasic stimuli compared to the homophasic stimuli indicates sensitivity of the brain towards for the phase difference in the applied stimuli. [21].
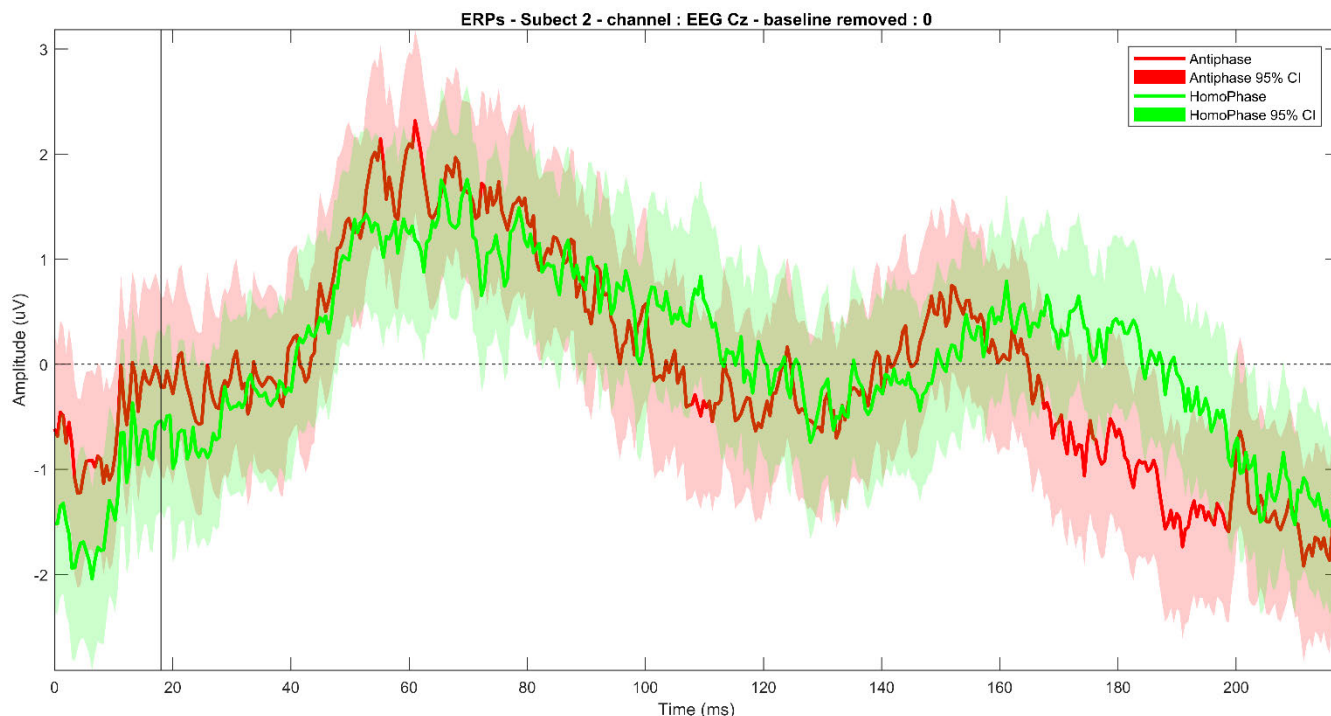
FIGURE 18. Time domain signals for a subject for both conditions for Cz channel.

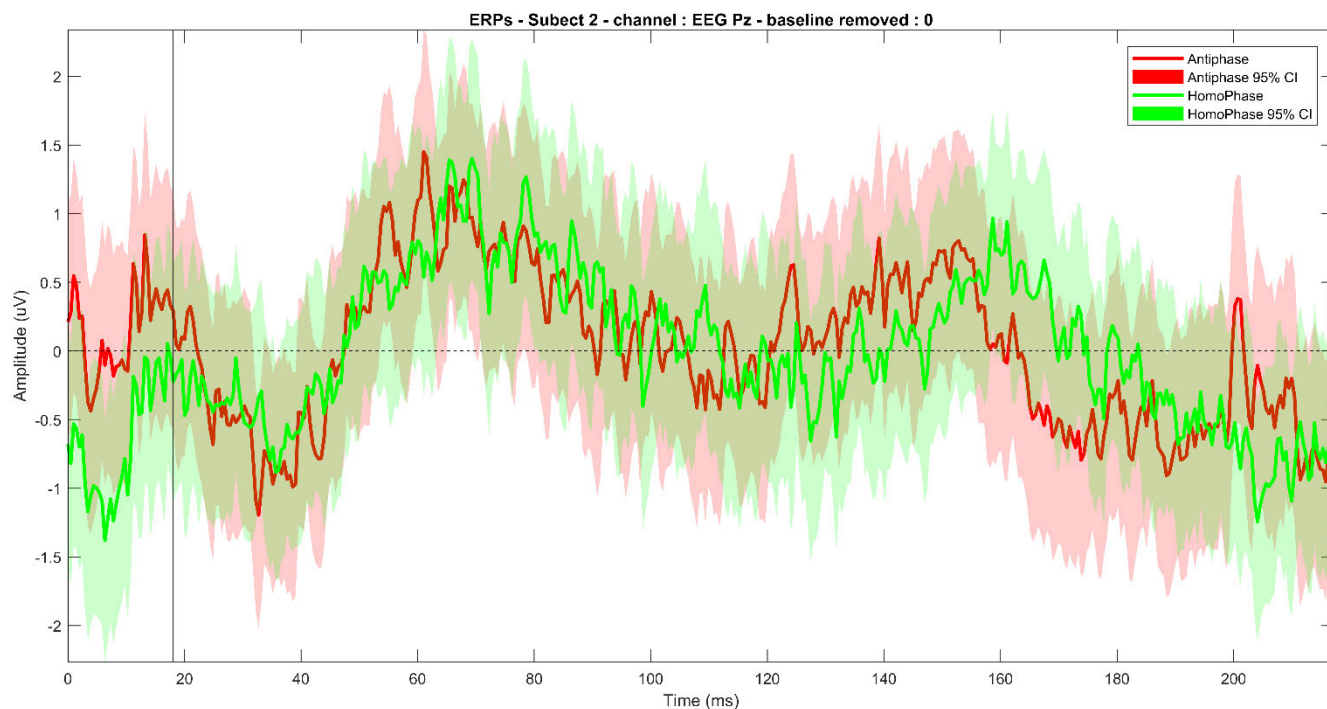**FIGURE 19.** Time domain signals for a subject for both conditions for Pz channel.

D. FREQUENCY DOMAIN ANALYSIS

For a better insight in the signal characteristics, the amplitudes and frequencies were found using the Fast Fourier Transform (FFT) [103] [21]. This is one of the best methods for determining the dominant frequencies in the signal and is also a numerically efficient technique for finding the various

TABLE 4. The difference in area under the time domain signals of the Cz and Pz channels for 9 subjects in both the conditions.

Energy under the time domain homophasic and Antiphasic signals from the Cz and Pz electrode locations

Subject	Cz_Area_Out	Cz_Area_In	Cz_ Area _Out-Cz_ Area _In	Pz_ Area _Out	Pz_ Area _In	Pz_ Area _Out-Pz_ Area _In
1	55.2299	36.40119	18.8288	50.0007	45.0996	4.9010
2	392.8738	230.2163	162.6575	127.4172	118.7825	8.6346
3	303.1516	130.6031	172.5485	292.9909	157.3418	135.6490
4	567.7618	365.1546	202.6072	275.1239	373.6057	-98.4818
5	192.9375	128.6475	64.2899	161.2470	46.6983	114.5487
6	191.9079	161.9911	29.9168	210.4534	135.2658	75.1876
7	221.7553	140.4256	81.3296	125.3709	74.7362	50.6347
8	214.9599	370.6023	-155.6423	78.3749	144.6907	-66.3154
9	442.7075	396.6837	46.0237	262.6003	218.8066	43.7937

Note: The green colour indicates a higher area for the antiphasic condition compared to the homophasic condition. The red colour represents vice versa condition.
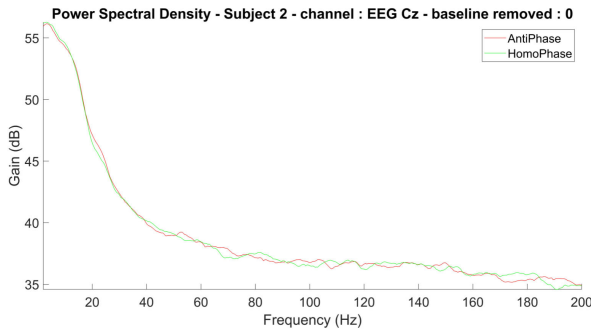
FIGURE 20. PSD for Cz channel.
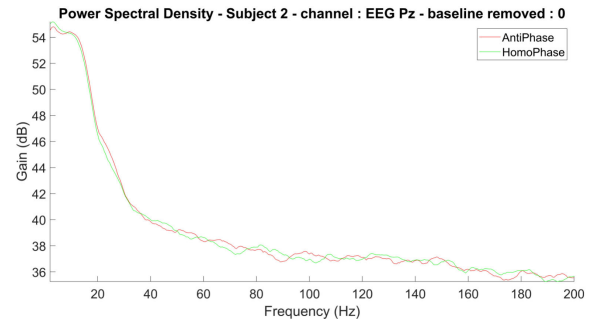
FIGURE 21. PSD for Pz channel.

frequency components of the EEG signal data [49]. The Fast Fourier Transform (FFT) was applied to the averaged epochs for both the antiphasic and homophasic data.

For a signal length n, FFT (Y) is given by

$$Y(k) = \sum_{j=1}^{n} X(j) W_n^{(j-1)(k-1)} \qquad (2)$$

where

$$W_n = e^{(-2\pi i)}/n \qquad (3)$$

The mean power spectral density over the trials of different subjects for both conditions was computed and plotted, see Figure 20 and Figure 21. The power spectral density (PSD) reflects the frequencies of interest in a signal. The PSD plots illustrate the distribution of the signal power vs frequency. This can also help in determining the state of activeness

and alertness for the subject under study as the frequency content of an EEG is affected by the level of alertness [39]. To obtain the Power Spectral Density (PSD) of the epochs, the following equation was used.

$$PSD = abs(FFT)^2 \qquad (4)$$

Figure 20 and 21 show the representative PSD plots for the channels Cz and Pz in EEG for one subject out of nine under study.

The PSD plots for different subjects elicited by homophasic and antiphasic stimuli indicate that most of the energy of the signal is contained in frequencies up to 150 Hz and that is gradually reduced with higher frequencies. The EEG signal generally lies within the range of 0.5 to 100 Hz for a human being [18]. However, the energy in frequencies from 80 Hz to 150 Hz represents the high gamma power EEG range which is strongly linked to selective attention [104].

TABLE 5. Energy per Frequency Band for ERP signals from the Cz Electrode Location.

Frequency Band	15 - 20		20 - 25		25 - 30		30 - 35		35 - 40		40 - 45	
	E-Out	E-In	E-Out	E-In	E-Out	E-In	E-Out	E-In	E-Out	E-In	E-Out	E-In
Subject	[dB]	[dB]	[dB]	[dB]	[dB]	[dB]	[dB]	[dB]	[dB]	[dB]	[dB]	[dB]
1	50.6068	50.7349	48.8272	48.3893	45.751	45.6315	42.8311	42.9158	40.8189	40.6241	39.3843	39.6911
2	49.1271	48.8594	46.0921	45.4465	43.3548	43.1596	41.6379	41.6472	40.5432	40.4697	39.5106	39.8386
3	53.2153	53.3288	51.4737	51.7013	50.6273	50.4652	49.7148	49.9930	48.3913	48.7567	47.272	47.6384
4	48.3772	48.0711	47.2072	46.8252	46.3437	45.5136	45.0116	44.7247	44.0555	43.8195	43.6672	43.5629
5	47.8745	47.8889	45.5367	45.1212	42.7295	42.4714	39.9803	40.2156	38.0674	38.4999	37.3458	37.5846
6	52.1943	52.0282	50.4489	50.0433	48.4498	48.1097	45.6442	45.6694	42.9443	43.0653	42.2001	42.0109
7	48.1888	47.9293	46.8969	46.5284	45.0799	45.0664	43.1594	43.2118	41.3480	41.6502	40.2558	40.5209
8	50.8100	50.5169	50.4078	49.8206	49.9418	49.3865	48.0397	47.5513	45.9343	45.5789	44.1577	43.7688
9	47.8048	48.1730	48.3939	48.2008	49.9124	49.4225	49.7260	49.6701	47.6513	47.5983	46.3714	45.8527

TABLE 6. Energy per Frequency Band for ERP signals from the Pz Electrode Location.

Frequency Band	15 - 20		20 - 25		25 - 30		30 - 35		35 - 40		40 - 45	
	E-Out	E-In	E-Out	E-In	E-Out	E-In	E-Out	E-In	E-Out	E-In	E-Out	E-In
Subject	[dB]	[dB]	[dB]	[dB]	[dB]	[dB]	[dB]	[dB]	[dB]	[dB]	[dB]	[dB]
1	51.2388	51.2003	48.3853	48.2921	44.7907	44.6726	42.1163	42.0447	40.1825	40.5136	39.1106	39.3792
2	49.7142	49.2019	45.9577	45.2507	43.5710	43.1570	41.2745	41.1219	40.2071	40.3341	39.5964	39.8790
3	52.9178	53.3990	51.4485	51.5505	50.5494	50.0927	49.7673	49.8115	48.8893	49.0515	47.7577	47.988
4	48.5665	48.5793	47.4025	47.4521	47.0928	46.4522	45.7617	45.2090	45.1872	44.6974	44.4929	44.1719
5	48.8576	48.2109	45.8725	45.2003	42.0145	41.7900	39.2612	39.6063	37.5844	38.3047	36.9636	37.3338
6	53.0794	52.8493	50.2664	50.4049	47.6527	47.7666	45.3536	45.5875	43.4319	43.8359	43.2108	42.8610
7	47.3021	47.2935	45.2291	44.8983	43.2565	43.2624	41.5165	41.4383	40.3757	40.2920	39.6898	39.4565
8	50.3974	50.4425	48.5602	48.0364	47.9396	47.5350	46.6019	46.1827	44.7949	44.4003	43.7780	43.4307
9	48.0412	47.8657	47.8182	46.9221	48.5685	47.6435	48.6577	48.1581	47.6351	47.2380	46.8017	46.3201

Combining the low frequency EEG with the high-power gamma activity could enhance resulting neural responses [105]. The frequency range also relates to the state of consciousness of a subject [39]. Frequencies below 15 Hz were not included at this stage as it is believed that the occurrence of alpha waves due to relaxation and possible temporary eye closure of some subjects might interfere with the mentioned frequency range [106], [107]. FFT analysis is used to compute the mean power per frequency band of interest. The energy analysis was carried out for six different frequency bands with frequencies, f, between 15Hz and 45Hz and a width of 5 Hz. Frequency bands include the lower frequency but not the higher frequency, so 15 – 20 Hz means that the frequency f is in the range of 15 Hz ≤ f < 20 Hz. This method is used to investigate whether there is a noticeable difference in the frequency range for both conditions. The energy for each frequency band is shown in Table 5 and 6.

E-out stands for energy in the antiphasic condition and E-in stands for energy in the homophasic condition respectively. The difference of the energy values for the two conditions in the different frequency bands was also tabulated, see Table 7 and 8.

The analysis of the energy spectrum data, shown in Tables 7 and 8shows that the frequency bands of 20 - 25Hz and 25 - 30Hz contain more energy for the antiphasic condition than for the homophasic condition. In Table 8 and 9, the green colour indicates a higher energy for the antiphasic condition compared to the homophasic condition for the frequency bands 20 - 25Hz and 25 - 30Hz. The red colour represents a higher energy in the homophasic condition. The frequency band analysis helps to find the frequency range where the difference for the binaural cue of phase reversal is maximal, which may be an indication of binaural processing. The larger energy in the antiphasic

TABLE 7. Energy difference for different Frequency Bands of ERP signals from the Cz Electrode Location.

Energy difference for different Frequency bands of ERP signals for Cz Channel						
Frequency Band	15 - 20	20 - 25	25 - 30	30 - 35	35 - 40	40 - 45
	E_Out-E_In	E_Out-E_In	E_Out-E_In	E_Out-E_In	E_Out-E_In	E_Out-E_In
Subject	[dB]	[dB]	[dB]	[dB]	[dB]	[dB]
1	-0.128111	0.437906	0.1195055	-0.084655	0.194877	-0.306836
2	0.2676988	0.645544	0.1951825	-0.009239	0.073506	-0.327939
3	-0.113497	-0.227619	0.1620546	-0.278207	-0.365336	-0.366416
4	0.3060296	0.381946	0.8301104	0.2869319	0.236081	0.1042928
5	-0.014399	0.415492	0.2581335	-0.235359	-0.432467	-0.238862
6	0.1660234	0.405614	0.3401152	-0.025176	-0.121045	0.1892007
7	0.2595292	0.368475	0.0135039	-0.052347	-0.302147	-0.265031
8	0.2930676	0.587196	0.5552608	0.4884534	0.355395	0.3889287
9	-0.368249	0.193028	0.4898973	0.0558702	0.052978	0.5186212

Note: The green colour indicates a higher energy for the antiphasic condition compared to the homophasic condition for the frequency bands 20-25Hz and 25-30Hz. The red colour represents a higher energy in the homophasic condition.

TABLE 8. Energy difference for different Frequency Bands of ERP signals from the Pz Electrode Location.

Energy difference for different Frequency bands of ERP signals for Pz Channel						
Frequency Band	15 - 20	20 - 25	25 - 30	30 - 35	35 - 40	40 - 45
	E_Out-E_In	E_Out-E_In	E_Out-E_In	E_Out-E_In	E_Out-E_In	E_Out-E_In
Subject	[dB]	[dB]	[dB]	[dB]	[dB]	[dB]
1	0.0384023	0.0931636	0.1181332	0.0716678	-0.331063	-0.26858
2	0.5122293	0.7070414	0.4139997	0.1525614	-0.127007	-0.282641
3	-0.481192	-0.101999	0.4566994	-0.0442446	-0.162255	-0.230293
4	-0.012805	-0.049558	0.6405954	0.5526312	0.4897514	0.3210298
5	0.6467357	0.6722349	0.2245513	-0.3451525	-0.720282	-0.370249
6	0.2300633	-0.13845	-0.113976	-0.2339086	-0.403966	0.3497353
7	0.0086224	0.3308032	-0.00587	0.0782094	0.0836896	0.2333681
8	-0.045117	0.5238104	0.4045682	0.4192029	0.3946276	0.3473045
9	0.1755287	0.8960823	0.9250097	0.4995631	0.3971102	0.4816445

Note: The green colour indicates a higher energy for the antiphasic condition compared to the homophasic condition for the frequency bands 20-25Hz and 25-30Hz. The red colour represents a higher energy in the homophasic condition.

condition compared to the homophasic support previous finding that the binaural cue of interaural phase difference (IPD) plays an important role in identifying the signal source.

E. STATISTICAL ANALYSIS

Statistical analysis was performed to evaluate the significance of the observed differences in the AEPs due to change in the phase of the stimulus. IBM SPSS Statistics 26 was used to perform the statistical analysis. Pairwise t-tests were used to evaluate differences between the Pz and Cz electrodes and their frequency bands. The basic equation for pairwise t-test where $\bar{d}$ is the mean difference between the paired groups,

s_d is the standard deviation of the differences and n the number of pairs is:

$$t = \frac{\bar{d}}{S_d/\sqrt{n}} \quad (5)$$

A Bonferroni correction was applied to compensate for the multiple comparison problem since a total of four comparisons was carried out for two electrode locations with the desired alpha ($\propto$) of 0.05. Additionally, a three-way ANOVA, with channels (Cz and Pz), stimulus (Antiphase and phase), and frequency (20-25 Hz and 25-30 Hz) as factors, was performed to evaluate any interaction effects in PSD. The statistical threshold for significance was set at $p < 0.05$.

TABLE 9. Pairwise t-test results.

Channel	Frequency (Hz)	Stimulus 1	Mean ± SD (standard deviation)	Stimulus 2	Mean ± SD (standard deviation)	t-test p-value	Significance
	20 - 25	Antiphasic	48.36 ± 2.09	Homophasic	48.01 ± 2.23	0.003	Yes
Cz	25 - 30	Antiphasic	46.91 ± 2.95	Homophasic	46.58 ± 2.88	0.005	Yes
	Mean ± SD	47.64 ± 2.59	-	47.29 ± 2.60	-	-	-
	20 - 25	Antiphasic	47.88 ± 2.07	Homophasic	47.56 ± 2.32	0.037	No
Pz	25 - 30	Antiphasic	46.16 ± 2.86	Homophasic	45.82 ± 2.74	0.014	No
	Mean ± SD	47.02 ± 2.58	-	46.69 ± 2.62	-	-	-

The equation for ANOVA in terms of linear regression is as follows:

$$
\begin{aligned}
Amp_{i,j} = {} & \beta_0 + \beta_1 * Channel_{i,j} + \beta_2 * Phase_{i,j} + \beta_3 \\
& * Frequency_{i,j} + \beta_4 * Channel_{i,j} \\
& * Phase_{i,j} + \beta_5 * Channel_{i,j} \\
& * Frequency_{i,j} + \beta_6 * Phase_{i,j} \\
& * Frequency_{i,j} + \beta_7 * Channel_{i,j} \\
& * Phase_{i,j} * Frequency_{i,j} + \varepsilon_{i,j}
\end{aligned}
\tag{6}
$$

where i is the subject number, j is the measurement number, channel is Cz when $Channel = 0$ and Fz when $Channel = 1$, phase is antiphase when $Phase = 1$ and homophase when $phase = 0$, frequency is 20-25 Hz when $Frequency = 1$ and 25-30 Hz when $Frequency = 0$.

The results from statistical analysis are shown in table 9. Here the frequency bands $20 - 25$ Hz and $25 - 30$ Hz resulted in a larger energy difference for antiphasic signals compared to homophasic signals for the Cz and Pz electrodes. Results for channel Cz show that there were significant differences between the response to the antiphasic and homophasic stimuli for both frequency bands ($20 - 25$ Hz and $25 - 30$ Hz).

While results for Cz are still significant, results for Pz, when the p-value was corrected for multiple comparisons (i.e., p-value > 0.0125), were no longer significant. This same trend was observed for the parametric (paired t-test) tests.

Similar results were shown by ANOVA (Table 10). As in the table 10, the ANOVA results indicate that there were no significant two-way and three-way interactions, but the main effects of the factors channel and frequency were significant ($p < 0.05$). The results of main effects which were also seen with the paired parametric test, show that there were significant differences between the responses at channel (Cz)
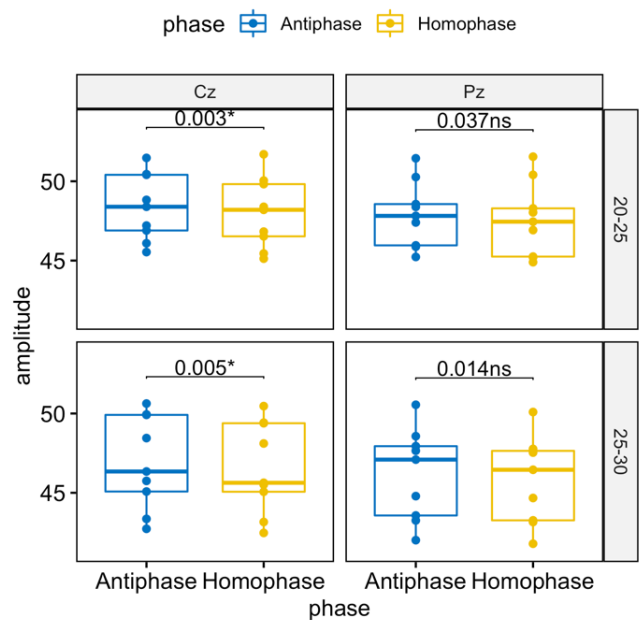

FIGURE 22. PSD boxplots and p-values for t-test. ∗ = significant differences; ns = non significant differences.

compared to channel (Pz). Figure 22 shows the boxplots and p values for parametric test. In box plots it can be seen that the median PSD amplitude for channel Pz is similar for the two stimuli phases, however, it is lower for homophase stimulus compared to antiphase stimulus in channel Cz. These differences were significant for the Cz channel for both the frequency ranges, but not for the channel Pz. Furthermore, the figure 22 shows that there are no outliers in the data as all the data points (shown as small circles in the box plots) are within ± 1.5∗interquartile range.

TABLE 10. ANOVA results.

Effect	F	df	df.res	*p-value*
channel	8.51	1	56	0.005
frequency	57.16	1	56	<0.001
phase	2.60	1	56	0.113
channel:frequency	0.47	1	56	0.494
channel:phase	0.00	1	56	0.982
frequency:phase	0.00	1	56	0.988
channel:frequency:phase	0.00	1	56	0.961

TABLE 11. Shapiro-Wilk normality test.

Channel	Phase	Frequency (Hz)	*p-value*
Cz	Anitphase	20-25	0.642
Cz	Homophase	20-25	0.762
Cz	Anitphase	25-30	0.396
Cz	Homophase	25-30	0.453
Pz	Anitphase	20-25	0.793
Pz	Homophase	20-25	0.415
Pz	Anitphase	25-30	0.676
Pz	Homophase	25-30	0.633

TABLE 12. Levene's test for homogeneity of variances.

Channel	Frequency (Hz)	*p-value*
Cz	20-25	0.900
Cz	25-30	0.905
Pz	20-25	0.744
Pz	25-30	0.895

We used ANOVA for the data as suggested in section 10.3.2 by Andy Field [108], since the group sizes are equal. ANOVA is neither affected by non-normality of the data distribution nor affected by non-homogeneous variances across groups, and therefore, is a robust method. Nonetheless, we tested for the normality of the data distribution using the Shaprio-Wilk normality test. The data was normally distributed as all $p > 0.05$ as shown in Table 11. Using Levene's test, we tested for the homogeneity of the variance across groups. The results showed that we can assume equal variances across groups as all $p > 0.05$ (Table 12). These results suggest using parametric methods for statistical testing.

IV. DISCUSSION

The study aims to analyse the AEP signals and the effect of phase change which can be indicative for binaural processing in the human brain. The analysis was carried out with a correlation study to identify the best channels for the AEP data acquisition. The findings and observations provide a strong contribution to the channel selection and the analysis methodology for the AEPs in detecting the phase change in the stimuli which in turn can indicate the sense of binaural hearing. Table 10 illustrates the important findings of our study.

The AEPs are analysed in different conditions to understand the response of brain towards the auditory stimuli. R.A. Utler in [109] studied the human cortical potentials evoked by a 1000 Hz tone in both monaural and binaural conditions. The results indicated a larger cortical response with increases of amplitude, area and latency for binaural stimulation compared to monaural stimuli. Similarly, in 1974 Picton [22] studied the components of the human auditory evoked potential, which can be recorded from the scalp and described the potential significance of the different peaks. P. Ungan *et al.* [110] measured binaural difference based on the ITD by using the chirp stimuli, ensuring a high SNR of the data. A systematic dependency of the amplitude and latency on the binaural difference was detected for individual subjects in the study. Similarly, to this study, we are studying the binaural sensitivity of the brain, however the difference

lies in the selection of stimuli with an interaural phase difference. The results from our study indicate that there are higher values for time domain and frequency domain features for antiphasic stimuli compared to homophasic ones which may be an indicative of binaural processing in the human brain. According to literature, the binaural cues ITD and ILD are used in studies of binaural sensitivity in hearing [111]–[114]. Sounds reaching the two ears are characterized by the binaural cues interaural time delay (ITD) or the related cue Interaural Phase Difference (IPD) as well as interaural level difference (ILD). As phase reversal can be considered a variant of IPD, this can be used to study the effect on AEPs. The higher amplitudes for r the antiphasic signals compared to the homophasic signals may be an indicator of binaural sensitivity. In 1936, Stevens [115] found that sound localization ability depends mainly on the ability to detect interaural time differences for low frequencies and interaural level differences for high frequencies. A time delay for a pure tone could be detected be detected because of the phase difference between the two ears. Ross B used the IPD cue to detect how binaural information is processed by the brain using MEG studies. Other studies also IPD stimuli in order to understand Auditory Evoked Responses from the brain [116]–[118].

Ross, Tremblay, & Picton (2007) [118] used the MEG P1-N1-P2 to study physiological detection of IPDs. They used a sinusoidal amplitude modulated tone (4.0 s in duration), with a stimulus onset asynchrony as stimulus in their study and introduced phase changes in different ears. They tried modulation to prevent the subject from perceiving a discontinuity in the sound. In our research we used the Blackmann windowing technique to remove the discontinuity. Their studies reveal the fact that the antiphasic signals (phase reversed ones) are able to provoke a larger impact on the Auditory Evoked Responses compared to the homophasic ones. Similar stimuli can be used to study the effect of AEP with EEG instead of MEG, as we have done in our study. When a ±180 interaural phase difference is applied in between left and right stimulus, the resulting components should gain a detectability. The difference in the choice of stimuli is that we have this without noise for better understanding of the neural activity towards the phase shifted stimuli.

The choice of frequency 500Hz for our study is based on literature where this has commonly been used to evaluate the auditory pathways [53], [97]. The selection of best electrode sites for EEG while studying the AEPs is also in agreement with literature [119]–[121], where Cz and other midline electrode locations were used for the analysis of AEPs from the scalp in response to auditory stimuli. Signals at the C region of the skull tend to be larger in amplitude than the signals in other regions [70]. However, the correlation analysis in our study suggests that the Pz location which lies in the midline of brain could also provide significant information on the binaural sensitivity. The analysis techniques in this study are based on the previous research and current methods.

The correlation technique used uses a similar methodology as described in [42], where they have tried to understand the correlation of EEG electrode locations with respect to the distance. We have used correlation technique to provide insight in the best EEG electrode locations for our study. Binaural studies described in literature commonly use time domain analysis [58], [109], [122]. A difference between previous studies and our method is the area calculation, indicating a higher energy for the response to antiphase signals, which could indicate binaural interaction in the human brain. In the spectral study using the FFT, the PSD plots provide the insight that most of the energy is in the range of 0.5 Hz to 100 Hz (EEG energy spectrum) and also that there is power in the gamma wave range, from 80 Hz to 150 Hz, which indicates selective attention while hearing sound stimuli with a phase difference [104], [105]. The frequency band wise analysis for homophasic and antiphasic signals shows that the frequency bands 20-25 Hz and 25-30 Hz had more energy when elicited by antiphasic stimuli compared to the homophasic condition. These frequency bands correspond to the Beta frequency range which may indicate conscious phase detection by the brain [37], [123]. The selection of the stimuli used for the study, the investigation for the most suitable electrode locations [72], [99] and frequency bands which can give an indication of the binaural interaction in the human brain [109], [124] and makes our current research relevant.

Based on the correlation study, the electrode locations Cz and Pz were selected for further analysis. The selection of electrode locations for AEP recording is in line with previous literature in which researchers selected the midline electrodes for the ERP analysis [72], [99]. A high correlation in these regions shows that these electrodes are highly correlated. Cz and Pz have better correlation to all other locations than other locations. The correlation analysis is mainly done for selection of the most suitable electrode indicated by better correlation with other positions. R Bhavsar et al [42], studied the relationship between different electrode locations to the distance and carried out the cross correlation analysis in the time domain. Their conclusion revealed the fact that correlation of electrical activity decreases with distance. However, this was not based on AEP's. We have performed a correlation study to identify the electrode locations that can also be considered as reflective of the AEP responses from other locations. With this process we were able to establish that Cz and Pz were the most correlated locations for responses to the auditory stimuli.

In time domain analysis of biosignals, the area under the curve can be analysed to understand differences in conditions or parameters and may also be used to extract features for further processing. In the review study of time domain analysis for EEG signals by V. K. Harpale [57] the area or energy under the time plots from different electrodes in EEG data has is mentioned as an indication of the synchronisation of signals. In our research, for the time domain analysis, the difference in the area under the antiphasic and homophasic

TABLE 13. Major findings of study.

Best Electrode Locations	• Cz, Pz
Time Domain Analysis	• Cz − 8 subjects out of 9, had a larger area in the antiphasic condition • Pz − 7 subjects out of 9 of subjects had a larger area in the antiphasic condition
Frequency Domain Analysis	• PSD plots − most energy below 150 Hz • Frequency bands 20 - 25Hz and 25 - 30Hz have larger energy when elicited by antiphasic stimuli for Cz and Pz electrode locations
Statistical Analysis	• Channel Cz shows significant differences between the response to the antiphasic and homophasic stimuli for both frequency bands (20 − 2 5Hz and 25 − 30 Hz) • Channel Pz results, when the p-value was corrected for multiple comparisons (i.e., p-value > 0.0125), were no longer significant.

conditions was determined. For the channel Cz, eight out of nine subjects had a larger area for the antiphasic condition compared to the homophasic condition. Seven subjects out of nine subjects had a larger area for the antiphasic condition than the homophasic condition for the Pz location. The time domain analysis involves the signal averaging and representation of the signals with respect to time for study of characteristics related to the ERPs. The correlation analysis and area under the curve for time domain represented signals provide an insight in the most representative electrode positions to study the effect of homophasic and antiphasic signals in AEPs in order to further understand binaural processing. The larger area for antiphasic signals compared to homophasic signals provide an indication that the AEPs can indicate the detection of binaural phase differences. The difference in the area for the homophasic and antiphasic signals suggests indication of binaural interaction of the brain.

In the spectral study using the FFT, the PSD plots provide the insight that most of the signal energy is in the range of 0.5 Hz to 100 Hz (EEG energy spectrum) and also power in the gamma wave range, from 80 Hz to 150 Hz, which indicates selective attention while hearing sound stimuli with a phase difference [104], [105]. The frequency band wise analysis for the homophasic and antiphasic signals show that the frequency bands 20 - 25Hz and 25 - 30Hz had more energy when elicited by antiphasic stimuli compared to the homophasic condition. The discussed frequency bands come under the beta band corresponding to the consciousness relating the phase detection by the brain [37], [123]. The findings corresponding to the Cz and PZ channels were further undergone statistical analysis separately to find the significance of the observations. The comparisons done with the Cz location showed statistically significant observations which in turn

support the importance of the Cz channel while making AEP studies from the EEG measurements [119]–[121].

In our research, we recruited nine number of subjects. The reverse result in Cz and Pz analysis for one of the subjects may be due to a difference in concentration levels. The other subject with larger area for homophasic condition at Pz was at the upper limit of our age criteria. Future work with larger numbers of subjects may further clarify possible reasons for different results.

V. CONCLUSION

The study analyses the AEP signals and the effect of phase change which may be a cue for binaural processing in the human brain. The electrode locations Cz and Pz were selected after the correlation for further analysis. In the time domain analysis, the channel Cz, eight out of nine subjects had a larger area for the antiphasic condition compared to the homophasic condition. Seven subjects out of nine subjects had a larger area for the antiphasic condition than the homophasic condition for the Pz location. This indicates that the difference in the area for the homophasic and antiphasic signals could be used for further research on binaural processing of the brain. The frequency bands 20 - 25Hz and 25 - 30Hz had more energy when elicited by antiphasic stimuli compared to the homophasic condition while performed the frequency domain analysis. The frequency bands of 20 - 25Hz and 25 - 30Hz in combination with the application of phase reversal of the auditory stimuli could be utilised in the development of an objective measurement of binaural hearing.

The applications of a hearing test using the AEPs allows for accurate testing and is independent of voluntary response from an individual under analysis. It is also useful in testing

infants or children with language disorders who may not give a reliable response. Moreover, an objective testing facility or methodology, which can detect binaural processing carried by the upper brain stem or the auditory cortex of the brain can be developed through the subsequent studies and experiments. According to prior research on hearing loss among children, binaural hearing problems due to different medical and environment conditions (for e.g.: otitis media) which are left untreated in the early stages, can adversely affect the child's development [7], [8]. The suggested research method could be used in developing objective methodology in detection of such hearing impairments. The difference in the AEP signals based on the phase change cue linked to the binaural hearing ability might help to make a step forward in diagnosing binaural processing disorders. Furthermore, the research is one of the attempts to find the effect of stimuli in homophase and antiphase conditions on the AEPs.

VI. LIMITATIONS OF THE STUDY

The current research attempts to find the effect of stimuli in homophasic and antiphasic stimuli in the ears and the resulting binaural (two-ear) interaction on the AEPs, however, there are some limitations. One limitation is the relatively small sample size. The fact that our study was limited to the electrode positions described above is another limitation. Future studies might address this. Our study is limited to homophasic and antiphasic stimuli at this stage. To further understand binaural processing expanding this to homophasic and antiphasic signals embedded in noise would be useful.

VII. FUTURE WORK

In the future, this study could be expanded to a larger number of subjects. Currently only subjects without any indications of hearing difficulties have been included. Including subject with (binaural) hearing difficulties would be a further step. A next step in our research will be using stimuli masked in noise and comparing AEPs with BMLD experiments which could provide further insight into binaural processing. Increasing the number of electrodes, including electrodes around the primary auditory area, such as TP, T, CP5/6, could lead to a further generalization of the study.

REFERENCES

[1] C. E. Dirks, *Using Binaural Beat Sensitivity to Describe Mechanisms That May Enhance Binaural Interactions in Single-Sided-Deafness Cochlear-Implant Patients*. Minneapolis, MN, USA: Univ. Minnesota, 2020.

[2] D. J. Breebaart, *Modeling Binaural Signal Detection*. Eindhoven, The Netherlands: Technische Universiteit Eindhoven, 2001.

[3] K. Dean and J. H. Grose, "The binaural interaction component of the auditory brainstem response under precedence effect conditions," *Trends Hearing*, vol. 24, Jan. 2020, Art. no. 233121652094613.

[4] B. Arons, "A review of the cocktail party effect," *J. Amer. Voice I/O Soc.*, vol. 12, no. 7, pp. 35–50, 1992.

[5] A. W. Bronkhorst, "The cocktail party phenomenon: A review of research on speech intelligibility in multiple-talker conditions," *Acta Acustica*, vol. 86, no. 1, pp. 117–128, 2000.

[6] P. B. Kishore, "Binaural hearing: Physiological and clinical view," *Arch. Otolaryngology Rhinology*, vol. 6, no. 2, pp. 33–36, May 2020.

[7] L. De Raeve, A. Vermeulen, and A. Snik, "Verbal cognition in deaf children using cochlear implants: Effect of unilateral and bilateral stimulation," *Audiology Neurotology*, vol. 20, no. 4, pp. 261–266, 2015.

[8] S. M. Misurelli, M. J. Goupell, E. A. Burg, R. Jocewicz, A. Kan, and R. Y. Litovsky, "Auditory attention and spatial unmasking in children with cochlear implants," *Trends Hearing*, vol. 24, Jan. 2020, Art. no. 233121652094698.

[9] C. Jolink, S. E. Lansbergen, and W. A. Dreschler, "Hearing disabilities and the effectiveness of rehabilitation in different age groups," *Otology Neurotology*, vol. 41, no. 8, pp. e982–e988, 2020.

[10] C. W. Newman, G. A. Hug, G. P. Jacobson, and S. A. Sandridge, "Perceived hearing handicap of patients with unilateral or mild hearing loss," *Ann. Otology, Rhinology Laryngology*, vol. 106, no. 3, pp. 210–214, Mar. 1997.

[11] N. Vannson, C. James, B. Fraysse, K. Strelnikov, P. Barone, O. Deguine, and M. Marx, "Quality of life and auditory performance in adults with asymmetric hearing loss," *Audiology Neurotology*, vol. 20, no. 1, pp. 38–43, 2015.

[12] M. Vander Ghinst, M. Bourguignon, M. Op de Beeck, V. Wens, B. Marty, S. Hassid, G. Choufani, V. Jousmäki, R. Hari, P. Van Bogaert, S. Goldman, and X. De Tiège, "Left superior temporal gyrus is coupled to attended speech in a cocktail-party auditory scene," *J. Neurosci.*, vol. 36, no. 5, pp. 1596–1606, Feb. 2016.

[13] N. Saadon-Grosman, S. Arzy, and Y. Loewenstein, "Hierarchical cortical gradients in somatosensory processing," *NeuroImage*, vol. 222, Nov. 2020, Art. no. 117257.

[14] C. J. M. Brian, "Hearing," in *Handbook of Perception and Cognition* 2nd ed. San Diego, CA, USA: Academic, 1995.

[15] D. Blackwood and W. Muir, "Cognitive brain potentials and their application," *Brit. J. Psychiatry*, vol. 157, no. S9, pp. 69–101, 1990.

[16] N. L. Maitre, A. P. Key, J. C. Slaughter, P. J. Yoder, M. L. Neel, C. Richard, M. T. Wallace, and M. M. Murray, "Neonatal multisensory processing in preterm and term infants predicts sensory reactivity and internalizing tendencies in early childhood," *Brain Topography*, vol. 33, no. 5, pp. 586–599, 2020.

[17] N. S. Williams, G. M. McArthur, B. de Wit, G. Ibrahim, and N. A. J. P. Badcock, "A validation of Emotiv EPOC Flex saline for EEG and ERP research," *PeerJ*, vol. 8, Aug. 2020, Art. no. e9713.

[18] E. Niedermeyer, D. L. Schomer, and F. H. L. da Silva, *Niedermeyer's Electroencephalography: Basic Principles, Clinical Applications, and Related Fields* (Electroencephalography), 6th ed. Philadelphia, PA, USA: Wolters, 2011.

[19] R. Hyder, A. Højlund, M. Jensen, K. Østergaard, and Y. Shtyrov, "Objective assessment of automatic language comprehension mechanisms in the brain: Novel E/MEG paradigm," *Psychophysiology*, vol. 57, no. 5, May 2020.

[20] S. Sur and V. Sinha, "Event-related potential: An overview," *Ind. Psychiatry J.*, vol. 18, no. 1, p. 70, 2009.

[21] T. W. Picton, *Human Auditory Evoked Potentials*. San Diego, CA, USA, Plural Publishing, 2010.

[22] T. W. Picton, S. A. Hillyard, H. I. Krausz, and R. Galambos, "Human auditory evoked potentials. I: Evaluation of components," *Electroencephalogr. Clin. Neurophysiol.*, vol. 36, pp. 179–190, Jan. 1974.

[23] A. Aroudi and S. Doclo, "Cognitive-driven binaural beamforming using EEG-based auditory attention decoding," *IEEE/ACM Trans. Audio, Speech, Language Process.*, vol. 28, pp. 862–875, 2020.

[24] D. Ibarra-Zarate and L. M. Alonso-Valerdi, "Acoustic therapies for tinnitus: The basis and the electroencephalographic evaluation," *Biomed. Signal Process. Control*, vol. 59, May 2020, Art. no. 101900.

[25] A. M. Proverbio, E. Camporeale, and A. Brusa, "Multimodal recognition of emotions in music and facial expressions," *Frontiers Hum. Neurosci.*, vol. 14, p. 32, Feb. 2020.

[26] B. Güntekin, H. Uzunlar, P. Çalışoğlu, F. Eroğlu-Ada, E. Yıldırım, T. Aktürk, E. Atay, and Ö. Ceran, "Theta and alpha oscillatory responses differentiate between six-to seven-year-old children and adults during successful visual and auditory memory encoding," *Brain Res.*, vol. 1747, Nov. 2020, Art. no. 147042.

[27] L. Soörnmo, *Bioelectrical Signal Processing in Cardiac and Neurological Applications*. Boston, MA, USA: Elsevier, 2005.

[28] A. Barman, P. Prabhu, V. G. Mekhala, K. Vijayan, and S. Narayanan, "Electrophysiological findings in specific language impairment: A scoping review," *Hearing, Balance Commun.*, vol. 19, no. 2, pp. 26–30, 2020.

[29] P. Marsella, A. Scorpecci, G. Cartocci, S. Giannantonio, A. G. Maglione, I. Venuti, A. Brizi, and F. Babiloni, "EEG activity as an objective measure of cognitive load during effortful listening: A study on pediatric subjects with bilateral, asymmetric sensorineural hearing loss," *Int. J. Pediatric Otorhinolaryngology*, vol. 99, pp. 1–7, Aug. 2017.

[30] R. L. I. Pillai, E. A. Bartlett, M. R. Ananth, C. Zhu, J. Yang, G. Hajcak, R. V. Parsey, and C. DeLorenzo, "Examining the underpinnings of loudness dependence of auditory evoked potentials with positron emission tomography," *NeuroImage*, vol. 213, Jun. 2020, Art. no. 116733.

[31] R. Markewitz, S. Engel, B. Langguth, and M. Schecklmann, "Effects of acoustic paired associative stimulation on late auditory evoked potentials," *Brain Topography*, vol. 32, no. 3, pp. 343–353, May 2019.

[32] V. Conde, L. Tomasevic, I. Akopian, K. Stanek, G. B. Saturnino, A. Thielscher, T. O. Bergmann, and H. R. Siebner, "The non-transcranial TMS-evoked potential is an inherent source of ambiguity in TMS-EEG studies," *NeuroImage*, vol. 185, pp. 300–312, Jan. 2019.

[33] H. Lee, D. Golkowski, D. Jordan, S. Berger, R. Ilg, J. Lee, G. A. Mashour, U. Lee, M. S. Avidan, S. Blain-Moraes, and G. Golmirzaie, "Relationship of critical dynamics, functional connectivity, and states of consciousness in large-scale human brain networks," *NeuroImage*, vol. 188, pp. 228–238, Mar. 2019.

[34] M. Seeber, L.-M. Cantonas, M. Hoevels, T. Sesia, V. Visser-Vandewalle, and C. M. Michel, "Subcortical electrophysiological activity is detectable with high-density EEG source imaging," *Nature Commun.*, vol. 10, no. 1, pp. 1–7, Dec. 2019.

[35] S. Baskar, V. S. Dhulipala, P. M. Shakeel, K. P. Sridhar, and R. Kumar, "Hybrid fuzzy based spearman rank correlation for cranial nerve palsy detection in MIoT environment," *Health Technol.*, vol. 10, no. 1, pp. 1–12, Jan. 2019.

[36] N. Coquelet, X. De Tiège, F. Destoky, L. Roshchupkina, M. Bourguignon, S. Goldman, P. Peigneux, and V. Wens, "Comparing MEG and high-density EEG for intrinsic functional connectivity mapping," *NeuroImage*, vol. 210, Apr. 2020, Art. no. 116556.

[37] T. Seifi Ala, M. A. Ahmadi-Pajouh, and A. M. Nasrabadi, "Cumulative effects of theta binaural beats on brain power and functional connectivity," *Biomed. Signal Process. Control*, vol. 42, pp. 242–252, Apr. 2018.

[38] A. K. Abbas, G. Azemi, S. Ravanshadi, and A. Omidvarnia, "An EEG-based methodology for the estimation of functional brain connectivity networks: Application to the analysis of newborn EEG seizure," *Biomed. Signal Process. Control*, vol. 63, Jan. 2021, Art. no. 102229.

[39] F. Cona, M. Zavaglia, L. Astolfi, F. Babiloni, and M. Ursino, "Changes in EEG power spectral density and cortical connectivity in healthy and tetraplegic patients during a motor imagery task," *Comput. Intell. Neurosci.*, vol. 2009, Jun. 2009, Art. no. 279515.

[40] V. Sakkalis, "Review of advanced techniques for the estimation of brain connectivity measured with EEG/MEG," *Comput. Biol. Med.*, vol. 41, no. 12, pp. 1110–1117, Dec. 2011.

[41] F. Wendling, K. Ansari-Asl, F. Bartolomei, and L. Senhadji, "From EEG signals to brain connectivity: A model-based evaluation of interdependence measures," *J. Neurosci. Methods*, vol. 183, no. 1, pp. 9–18, Sep. 2009.

[42] R. Bhavsar, Y. Sun, N. Helian, N. Davey, D. Mayor, and T. Steffert, "The correlation between EEG signals as measured in different positions on scalp varying with distance," *Procedia Comput. Sci.*, vol. 123, pp. 92–97, Jan. 2018.

[43] J. D. Bonita, L. C. C. Ambolode, B. M. Rosenberg, C. J. Cellucci, T. A. A. Watanabe, P. E. Rapp, and A. M. Albano, "Time domain measures of inter-channel EEG correlations: A comparison of linear, non-parametric and nonlinear measures," *Cognit. Neurodyn.*, vol. 8, no. 1, pp. 1–15, Feb. 2014.

[44] J. S. Lee, C. M. Han, J. H. Kim, and K. S. Park, "Reverse-curve-arch-shaped dry EEG electrode for increased skin–electrode contact area on hairy scalps," *Electron. Lett.*, vol. 51, no. 21, pp. 1643–1645, Oct. 2015. [Online]. Available: https://digital-library.theiet.org/content/journals/10.1049/el.2015.1873

[45] R. Zhang, P. Xu, T. Liu, Y. Zhang, L. Guo, P. Li, and D. Yao, "Local temporal correlation common spatial patterns for single trial EEG classification during motor imagery," *Comput. Math. Methods Med.*, vol. 2013, pp. 1–7, Nov. 2013.

[46] M. Hoffmann, "The human frontal lobes and frontal network systems: An evolutionary, clinical, and treatment perspective," *ISRN Neurol.*, vol. 2013, Mar. 2013, Art. no. 892459.

[47] M. R. Borich, S. M. Brodie, W. A. Gray, S. Ionta, and L. A. Boyd, "Understanding the role of the primary somatosensory cortex: Opportunities for rehabilitation," *Neuropsychologia*, vol. 79, pp. 246–255, Dec. 2015.

[48] D. J. Strauss, W. Delb, and P. K. Plinkert, "Analysis and detection of binaural interaction in auditory evoked brainstem responses by time-scale representations," *Comput. Biol. Med.*, vol. 34, no. 6, pp. 461–477, Sep. 2004.

[49] P. M. Pandiyan, K. Subramaniam, Y. Sazali, A. Hamid, P. Adom, and C. R. Hema, "EEG based detection of conductive and sensorineural hearing loss using artificial neural networks," *J. Next Gener. Inf. Technol.*, vol. 4, no. 3, pp. 204–212, May 2013.

[50] A. Kumar, S. Anand, and L. N. Yaddanapudi, "Comparison of auditory evoked potential parameters for predicting clinically anaesthetized state," *Acta Anaesthesiologica Scandinavica*, vol. 50, pp. 1139–1144, Jan. 2006.

[51] S. A. Hillyard, R. F. Hink, V. L. Schwent, and T. W. Picton, "Electrical signs of selective attention in the human brain," *Science*, vol. 182, no. 4108, pp. 177–180, Oct. 1973.

[52] S. Gupta, S. Mittal, A. Kumar, K. Singh, R. Sharma, and P. Baweja, "Analysis of gender based differences in auditory evoked potentials among healthy elderly population," *Adv. Biomed. Res.*, vol. 3, no. 1, p. 208, 2014.

[53] M. Emre Cek, M. Ozgoren, and F. Acar Savaci, "Continuous time wavelet entropy of auditory evoked potentials," *Comput. Biol. Med.*, vol. 40, no. 1, pp. 90–96, Jan. 2010.

[54] M. P. Paulraj, S. B. Yaccob, A. H. B. Adom, K. Subramaniam, and C. R. Hema, "EEG based hearing threshold diagnosis using feed-forward network," in *Proc. 7th Int. Conf. Intell. Syst. Control (ISCO)*, Jan. 2013, pp. 197–200.

[55] R. A. Dobie and M. J. Wilson, "Analysis of auditory evoked potentials by magnitude-squared coherence," *Ear Hearing*, vol. 10, no. 1, pp. 2–13, Feb. 1989.

[56] X. Gao, H. Cao, D. Ming, H. Qi, X. Wang, X. Wang, R. Chen, and P. Zhou, "Analysis of EEG activity in response to binaural beats with different frequencies," *Int. J. Psychophysiol.*, vol. 94, no. 3, pp. 399–406, Dec. 2014.

[57] V. K. Harpale and V. K. Bairagi, "Time and frequency domain analysis of EEG signals for seizure detection: A review," in *Proc. Int. Conf. Microelectron., Comput. Commun. (MicroCom)*, Jan. 2016, pp. 1–6.

[58] C. S. Herrmann, S. Rach, J. Vosskuhl, and D. Strüber, "Time–Frequency analysis of event-related potentials: A brief tutorial," *Brain Topography*, vol. 27, no. 4, pp. 438–450, Jul. 2014.

[59] S. A. F. Stehlin, X. P. Nguyen, and M. H. Niemz, "EEG with a reduced number of electrodes: Where to detect and how to improve visually, auditory and somatosensory evoked potentials," *Biocybern. Biomed. Eng.*, vol. 38, no. 3, pp. 700–707, 2018.

[60] N. Das, A. Bertrand, and T. Francart, "EEG-based auditory attention detection: Boundary conditions for background noise and speaker positions," *J. Neural Eng.*, vol. 15, no. 6, Dec. 2018, Art. no. 066017.

[61] S. Azam, T. Brown, M. Jonkman, and F. De Boer, "Effect of stimulus phase reversal on the 20–35 Hz frequency component of the AEP," in *Proc. 4th Int. Conf. Biomed. Eng. Informat. (BMEI)*, Oct. 2011, pp. 725–729.

[62] C. Guger, G. Edlinger, and G. Krausz, "Hardware/software components and applications of BCIs," in *Recent Advances in Brain-Computer Interface Systems*. Rijeka, Croatia: InTech, Feb. 2011, ch. 1, doi: 10.5772/14174.

[63] K. E. Mathewson, T. J. L. Harrison, and S. A. D. Kizuk, "High and dry? Comparing active dry EEG electrodes to active and passive wet electrodes," *Psychophysiology*, vol. 54, no. 1, pp. 74–82, Jan. 2017.

[64] P. Ledwidge, J. Foust, and A. Ramsey, "Recommendations for developing an EEG laboratory at a primarily undergraduate institution," *J. Undergraduate Neurosci. Educ.*, vol. 17, no. 1, pp. A10–A19, 2018.

[65] I. A. Ibrahim, H.-N. Ting, and M. Moghavvemi, "The effects of audio stimuli on auditory-evoked potential in normal hearing Malay adults," *Int. J. Health Sci.*, vol. 12, no. 5, pp. 25–34, Oct. 2018.

[66] S. Azam, T. Brown, M. Jonkman, and F. De Boer, "An acquisition method for the MLR of auditory evoked potentials," in *Proc. 4th Int. Conf. Biomed. Eng. Informat. (BMEI)*, Oct. 2011, pp. 1036–1040.

[67] H. L. M. Andrew and K. G. Athanasios, *10-20 EEG Placement*. Lausanne, Switzerland: European Respiratory Society (ERS), 2016.

[68] C. Elberling, S. G. B. Kristensen, and M. Don, "Auditory brainstem responses to chirps delivered by different insert earphones," *J. Acoust. Soc. Amer.*, vol. 131, no. 3, pp. 2091–2100, Mar. 2012.

[69] A. B. Usakli, "Improvement of EEG signal acquisition: An electrical aspect for state of the art of front end," *Comput. Intell. Neurosci.*, vol. 2010, pp. 1–7, Jan. 2010.

[70] C. Alain, S. R. Arnott, S. Hevenor, S. Graham, and C. L. Grady, "'What' and 'where' in the human auditory system," *Proc. Nat. Acad. Sci. USA*, vol. 98, pp. 12301–12306, Jan. 2001.

[71] G. Plourde, "Auditory evoked potentials," *Best Pract. Res. Clin. Anaesthesiology*, vol. 20, no. 1, pp. 129–139, 2006.

[72] S. L. Bell, D. C. Smith, R. Allen, and M. E. Lutman, "Recording the middle latency response of the auditory evoked potential as a measure of depth of anaesthesia. A technical note," *Brit. J. Anaesthesia*, vol. 92, no. 3, pp. 442–445, Mar. 2004.

[73] J.-Y. Jung, H.-Y. Cho, and C.-K. Kang, "Brain activity during a working memory task in different postures: An EEG study," *Ergonomics*, vol. 63, no. 11, pp. 1359–1370, 2020.

[74] N. M. Armstrong, P. H. Croll, B. C. Oosterloo, F. R. Lin, M. A. Ikram, A. Goedegebure, and M. W. Vernooij, "Association of speech recognition thresholds with brain volumes and white matter microstructure: The rotterdam study," *Otology Neurotology*, vol. 41, no. 9, pp. 1202–1209, Oct. 2020.

[75] O. Sporns, G. Tononi, and R. Kötter, "The human connectome: A structural description of the human brain," *PLoS Comput. Biol.*, vol. 1, no. 4, p. e42, 2005.

[76] T. Goossens, C. Vercammen, J. Wouters, and A. van Wieringen, "The association between hearing impairment and neural envelope encoding at different ages," *Neurobiol. Aging*, vol. 74, pp. 202–212, Feb. 2019.

[77] M. Van Eeckhoutte, J. Wouters, and T. Francart, "Objective binaural loudness balancing based on 40-Hz auditory steady-state responses. Part I: Normal hearing," *Trends Hearing*, vol. 22, Jan. 2018, Art. no. 2331216518805352.

[78] D. Tomé, F. Barbosa, K. Nowak, and J. Marques-Teixeira, "The development of the n1 and n2 components in auditory oddball paradigms: A systematic review with narrative analysis and suggested normative values," *J. Neural Transmiss.*, vol. 122, no. 3, pp. 375–391, Mar. 2015.

[79] T. Nakamura, T. H. Dinh, M. Asai, H. Nishimaru, J. Matsumoto, Y. Takamura, E. Hori, S. Honda, H. Yamada, T. Mihara, M. Matsumoto, and H. Nishijo, "Non-invasive electroencephalographical (EEG) recording system in awake monkeys," *Heliyon*, vol. 6, no. 5, May 2020, Art. no. e04043.

[80] B. I. Turetsky, J. Raz, and G. Fein, "Noise and signal power and their effects on evoked potential estimation," *Electroencephalogr. Clin. Neurophysiol./Evoked Potentials Sect.*, vol. 71, no. 4, pp. 310–318, Jul. 1988.

[81] W. T. Roth, P. L. Krainz, J. M. Ford, J. R. Tinklenberg, R. M. Rothbart, and B. S. Kopell, "Parameters of temporal recovery of the human auditory evoked potential," *Electroencephalogr. Clin. Neurophysiol.*, vol. 40, no. 6, pp. 623–632, Jun. 1976.

[82] A. Pfefferbaum, W. T. Roth, J. R. Tinklenberg, M. J. Rosenbloom, and B. S. Kopell, "The effects of ethanol and meperidine on auditory evoked potentials," *Drug Alcohol Dependence*, vol. 4, no. 5, pp. 371–380, Sep. 1979.

[83] S. K. Salo, A. H. Lang, A. J. Salmivalli, R. K. Johansson, and M. S. Peltola, "Contralateral white noise masking affects auditory N1 and P2 waves differently," *J. Psychophysiol.*, vol. 17, no. 4, pp. 189–194, Jan. 2003.

[84] A. Bahmer, O. Peter, and U. Baumann, "Recording of electrically evoked auditory brainstem responses (E-ABR) with an integrated stimulus generator in MATLAB," *J. Neurosci. Methods*, vol. 173, no. 2, pp. 306–314, Aug. 2008.

[85] K. Wilson and J. H. Korn, "Attention during lectures: Beyond ten minutes," *Teaching Psychol.*, vol. 34, no. 2, pp. 85–89, Apr. 2007.

[86] A. R. Absalom, N. Sutcliffe, and G. N. C. Kenny, "Effects of the auditory stimuli of an auditory evoked potential system on levels of consciousness, and on the bispectral index," *Brit. J. Anaesthesia*, vol. 87, no. 5, pp. 778–780, Nov. 2001.

[87] P. Sörqvist and J. E. Marsh, "How concentration shields against distraction," *Current Directions Psychol. Sci.*, vol. 24, no. 4, pp. 267–272, Aug. 2015.

[88] A. Bednar and E. C. Lalor, "Neural tracking of auditory motion is reflected by delta phase and alpha power of EEG," *NeuroImage*, vol. 181, pp. 683–691, Nov. 2018.

[89] H. Zavala-Fernández, R. Orglmeister, L. Trahms, and T. H. Sander, "Identification enhancement of auditory evoked potentials in EEG by epoch concatenation and temporal decorrelation," *Comput. Methods Programs Biomed.*, vol. 108, no. 3, pp. 1097–1105, Dec. 2012.

[90] A. de Cheveigné and D. Arzounian, "Robust detrending, rereferencing, outlier detection, and inpainting for multichannel data," *NeuroImage*, vol. 172, pp. 903–912, May 2018.

[91] J. van Driel, C. N. L. Olivers, and J. J. Fahrenfort, "High-pass filtering artifacts in multivariate classification of neural time series data," *J. Neurosci. Methods*, vol. 352, Mar. 2021, Art. no. 109080.

[92] D. Vernon, G. Peryer, J. Louch, and M. Shaw, "Tracking EEG changes in response to alpha and beta binaural beats," *Int. J. Psychophysiol.*, vol. 93, no. 1, pp. 134–139, Jul. 2014.

[93] P. Prado-Gutierrez, E. Martínez-Montes, A. Weinstein, and M. Zañartu, "Estimation of auditory steady-state responses based on the averaging of independent EEG epochs," *PLoS ONE*, vol. 14, no. 1, Jan. 2019, Art. no. e0206018.

[94] A.-K. Becher, M. Höhne, N. Axmacher, L. Chaieb, C. E. Elger, and J. Fell, "Intracranial electroencephalography power and phase synchronization changes during monaural and binaural beat stimulation," *Eur. J. Neurosci.*, vol. 41, no. 2, pp. 254–263, Jan. 2015.

[95] X. Jiang, G.-B. Bian, and Z. Tian, "Removal of artifacts from EEG signals: A review," *Sensors*, vol. 19, no. 5, p. 987, Feb. 2019.

[96] S. Sanei, *EEG Signal Processing*. Hoboken, NJ, USA: Wiley, 2007.

[97] F. Denk, M. Grzybowski, S. M. A. Ernst, B. Kollmeier, S. Debener, and M. G. Bleichner, "Event-related potentials measured from in and around the ear electrodes integrated in a live hearing device for monitoring sound perception," *Trends Hearing*, vol. 22, Jan. 2018, Art. no. 233121651878821.

[98] S. Rosemann, D. Smith, M. Dewenter, and C. M. Thiel, "Age-related hearing loss influences functional connectivity of auditory cortex for the McGurk illusion," *Cortex*, vol. 129, pp. 266–280, Aug. 2020.

[99] A. Bednar, F. M. Boland, and E. C. Lalor, "Different spatio-temporal electroencephalography features drive the successful decoding of binaural and monaural cues for sound localization," *Eur. J. Neurosci.*, vol. 45, no. 5, pp. 679–689, Mar. 2017.

[100] A. M. Ewan, D. S. Brian, and A. Guillaume, "How and why does spatial-hearing ability differ among listeners? What is the role of learning and multisensory interactions," *Frontiers Neurosci.*, vol. 10, p. 36, Feb. 2016.

[101] T. Lu, R. Litovsky, and F.-G. Zeng, "Binaural masking level differences in actual and simulated bilateral cochlear implant listeners," *J. Acoust. Soc. Amer.*, vol. 127, no. 3, pp. 1479–1490, Mar. 2010.

[102] B. Van Dun, J. Wouters, and M. Moonen, "Optimal electrode selection for multi-channel electroencephalogram based detection of auditory steady-state responses," *J. Acoust. Soc. Amer.*, vol. 126, no. 1, pp. 254–268, Jul. 2009.

[103] C. G. Clinard, S. L. Hodgson, and M. E. Scherer, "Neural correlates of the binaural masking level difference in human frequency-following responses," *J. Assoc. Res. Otolaryngology*, vol. 18, no. 2, pp. 355–369, Apr. 2017.

[104] S. Ray, E. Niebur, S. S. Hsiao, A. Sinai, and N. E. Crone, "High-frequency gamma activity (80–150Hz) is increased in human cortex during selective attention," *Clin. Neurophysiol.*, vol. 119, no. 1, pp. 116–133, Jan. 2008.

[105] S. R. Synigal, E. S. Teoh, and E. C. Lalor, "Including measures of high gamma power can improve the decoding of natural speech from EEG," *Frontiers Hum. Neurosci.*, vol. 14, Apr. 2020, Art. no. 785881.

[106] S. Nakamura, N. Sadato, T. Oohashi, E. Nishina, Y. Fuwamoto, and Y. Yonekura, "Analysis of music–brain interaction with simultaneous measurement of regional cerebral blood flow and electroencephalogram beta rhythm in human subjects," *Neurosci. Lett.*, vol. 275, no. 3, pp. 222–226, Nov. 1999.

[107] R. Srinivasan and P. L. Nunez, "Electroencephalography," in *Reference Module in Neuroscience and Biobehavioral Psychology*. Amsterdam, The Netherlands: Elsevier, 2017.

[108] A. Unwin, *Discovering Statistics Using R by Andy Field, Jeremy Miles, Zoë Field*. Hoboken, NJ, USA: Wiley, 2013.

[109] R. A. Utler, W. D. Keidel, and M. Spreng, "An investigation of the human cortical evoked potential under conditions of monaural and binaural stimulation," *Acta Otolaryngol*, vol. 68, no. 4, pp. 317–326, Oct. 1969.

[110] P. Ungan, S. Yağcioğlu, and B. Özmen, "Interaural delay-dependent changes in the binaural difference potential in cat auditory brainstem response: Implications about the origin of the binaural interaction component," *Hearing Res.*, vol. 106, nos. 1–2, pp. 66–82, Apr. 1997.

[111] H. Steven Colburn, B. Shinn-Cunningham, J. G. Kidd, and N. Durlach, "The perceptual consequences of binaural hearing," *Int. J. Audiology*, vol. 45, no. sup1, pp. 34–44, Jan. 2006.

[112] M. A. Akeroyd, "The psychoacoustics of binaural hearing," *Int. J. Audiology*, vol. 45, no. sup1, pp. 25–33, Jan. 2006.

[113] B. W. Johnson and M. J. Hautus, "Processing of binaural spatial information in human auditory cortex: Neuromagnetic responses to interaural timing and level differences," *Neuropsychologia*, vol. 48, no. 9, pp. 2610–2619, Jul. 2010.

[114] A. Kan and R. Y. Litovsky, "Binaural hearing with electrical stimulation," *Hearing Res.*, vol. 322, pp. 127–137, Apr. 2015.

[115] S. S. Stevens and E. B. Newman, "The localization of actual sources of sound," *Amer. J. Psychol.*, vol. 48, no. 2, pp. 297–306, 1936.

[116] B. Ross, T. Fujioka, K. L. Tremblay, and T. W. Picton, "Aging in binaural hearing begins in mid-life: Evidence from cortical auditory-evoked responses to changes in interaural phase," *J. Neurosci.*, vol. 27, no. 42, pp. 11172–11178, Oct. 17 2007.

[117] B. Ross, K. L. Tremblay, and T. W. Picton, "Physiological detection of interaural phase differences," *J. Acoust. Soc. Amer.*, vol. 121, no. 2, pp. 1017–1027, Feb. 2007.

[118] K. Tremblay and B. Ross, "Effects of age and age-related hearing loss on the brain," *J. Commun. Disorders*, vol. 40, no. 4, pp. 305–312, Jul. 2007.

[119] S. J. Oppitz, D. D. Didoné, D. D. da Silva, M. Gois, J. Folgearini, G. C. Ferreira, and M. V. Garcia, "Long-latency auditory evoked potentials with verbal and nonverbal stimuli," *Brazilian J. Otorhinolaryngology*, vol. 81, no. 6, pp. 647–652, Nov. 2015.

[120] M. A. Papesh, R. L. Folmer, and F. J. Gallun, "Cortical measures of binaural processing predict spatial release from masking performance," *Frontiers Hum. Neurosci.*, vol. 11, p. 124, Mar. 2017.

[121] L. V. Parry, M. R. D. Maslin, R. Schaette, D. R. Moore, and K. J. Munro, "Increased auditory cortex neural response amplitude in adults with chronic unilateral conductive hearing impairment," *Hearing Res.*, vol. 372, pp. 10–16, Feb. 2019.

[122] A. F. Gill, S. A. Fatima, A. Nawaz, A. Nasir, M. U. Akram, S. G. Khawaja, and S. Ejaz, "Time domain analysis of EEG signals for detection of epileptic seizure," in *Proc. IEEE Symp. Ind. Electron. Appl. (ISIEA)*, Sep. 2014, pp. 32–35.

[123] A. H. Ghaderi, S. Moradkhani, A. Haghighatfard, F. Akrami, Z. Khayyer, and F. Balcı, "Time estimation and beta segregation: An EEG study and graph theoretical approach," *PLoS ONE*, vol. 13, no. 4, Apr. 2018, Art. no. e0195380.

[124] R. A. Dobie and S. J. Norton, "Binaural interaction in human auditory evoked potentials," *Electroencephalogr. Clin. Neurophysiol.*, vol. 49, nos. 3–4, pp. 303–313, Aug. 1980.

SAMI AZAM (Member, IEEE) is currently a Leading Researcher and a Senior Lecturer with the College of Engineering, IT and Environment, Charles Darwin University, Australia. He has number of publications in peer-reviewed journals and international conference proceedings. His research interests include computer vision, signal processing, artificial intelligence, and biomedical engineering.

MIRJAM JONKMAN (Member, IEEE) is currently a Lecturer and a Researcher with the College of Engineering, IT and Environment. Her research interests include biomedical engineering, signal processing, and the application of computer science to real life problems.

EVA IGNATIOUS is currently a Ph.D. Researcher with Charles Darwin University, Australia. She has considerable research experience with one U.S. patent and two Indian patents for the development of thermal sensor-based breast cancer detection at its early stages together with the Centre for Materials for Electronics Technology (C-MET), an Autonomous Scientific Society under the Ministry of Electronics and Information Technology (MeitY), Government of India. Her research interests include biomedical signal processing (interesting features and abnormalities found in bio-signals), theoretical modeling and simulation (breast cancer tissues), applied electronics (thermistors), process control and instrumentation, and embedded/VLSI systems.

FRISO DE BOER is currently a Professor with the College of Engineering, IT and Environment, Charles Darwin University, Australia. His research interests include signal processing, biomedical engineering, and mechatronics.

• • •